

**2014 Spring**

**“Advanced Physical Metallurgy”  
- Bulk Metallic Glasses -**

**04.29.2014**

**Eun Soo Park**

**Office: 33-313**

**Telephone: 880-7221**

**Email: [espark@snu.ac.kr](mailto:espark@snu.ac.kr)**

**Office hours: by appointment**

# 4 *Synthesis of Bulk Metallic Glasses*

**Metallic glasses:** produced by rapidly solidifying metallic melts to cooling rate **about  $10^6$  K/s**



**BMG :** Produced by relatively slow solidification rates of **about  $10^3$  K/s or less**

## 4.2 Principles of Rapid Solidification Processing: Huge departure from equilibrium

- 1) A small quantity of the molten metal is ejected using a shock wave on to a conducting substrate. The molten metal spreads in the form of a thin layer, typically a few tens of micrometers (but usually about 20-50  $\mu\text{m}$ ) in thickness, and the heat is extracted rapidly by conducting copper substrate.
- 2) Basic requirements to achieve high solidification rates:
  - a. Forming a thin layer (film or ribbon) of the molten metal
  - b. Intimate thermal contact with a good heat-conducting substrate to rapidly extract the heat from the liquid metal

3)

$$R = \frac{A}{x^2}$$

where

$x$  is the distance from the splat/substrate interface

the constant  $A$  is a function of the material properties and initial temperatures, but is independent of  $x$

The value of  $A$  is  $8.1 \times 10^{-3} \text{ m}^2 \text{ K s}^{-1}$  for ideal cooling (when the heat transfer coefficient is  $\infty$ ) and it is less for nonideal cooling conditions. For example, assuming an average value of  $A = 10^{-3} \text{ m}^2 \text{ K s}^{-1}$ , for rough estimates, the solidification rate achieved will be approximately  $10^5 \text{ K s}^{-1}$  for  $x = 100 \mu\text{m}$  and  $10^9 \text{ K s}^{-1}$  for  $x = 1 \mu\text{m}$ . The typical thickness of a rapidly solidified foil is about  $50 \mu\text{m}$ , and therefore the foil would have solidified at a rate of approximately  $10^6 \text{ K s}^{-1}$ . These examples serve to illustrate that it is necessary to have as small a section thickness as possible to achieve high solidification rates.

### 4.3 General Techniques to Achieve High Rates of Solidification

“Energize and quench” – increase the free energy of the system (by either raising the temperature, or pressure or the input of mechanical energy, or by other means) and subsequently quenching the material to either retain the metastable phase or to use it as an intermediate step to achieve the desired microstructure and/or properties → Some very interesting properties

**4.4 Melt Spinning:** the most commonly used method to produce long and continuous rapidly solidified ribbons, wires, and filaments

- Free flight melt-spinning, Chill block melt-spinning  
: a small quantity of the alloy is melted inside a crucible or by levitation methods, and then ejected by pressurization through a fine nozzle onto a fast-rotating copper wheel.

- **Crucible material:** based on its chemical compatibility with the melts, its temperature handling capability, its resistance to thermal shock, its low thermal conductivity, and its low porosity (e.g. dense alumina and quartz)

- **Nozzle:** about 50  $\mu\text{m}$  to 1250  $\mu\text{m}$ , alumina, graphite, SiC, Sapphire, and pyrex glass

- **Ejection pressures:** 5-70 kPa depending on desired melt delivery rate, high ejection pressures → improvement of the wetting pattern and better thermal contact between the melt puddle and the substrate.

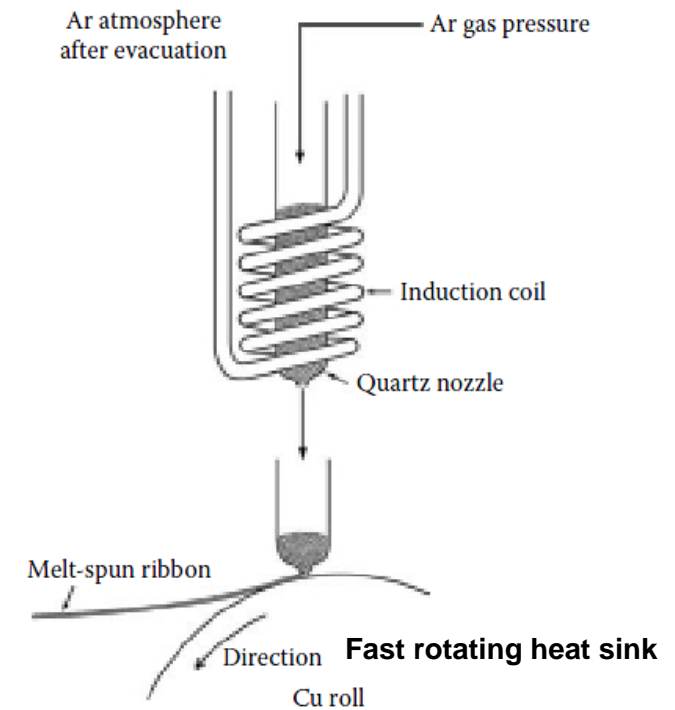


FIGURE 4.1  
Schematic illustration of the melt-spinning process.

#### 4.4 Melt Spinning: the most commonly used method to produce long and continuous rapidly solidified ribbons, wires, and filaments

##### - Wheel for melt-spinning:

- a) extract the heat from the ribbon as quickly as possible
- b) a variety of materials including copper, stainless steel, chromium, and molybdenum
- c) outer surface of the wheel is generally polished to remove any surface roughness  
due to wheel side of the cast ribbon → almost an exact replica of the wheel surface
- d) Wheel speed is an important parameter in determining the thickness of the ribbon  
ex\_  $\text{Fe}_{40}\text{Ni}_{40}\text{B}_{20}$  alloy, 250 mm diameter copper wheel,  
substrate velocity o 26.6 m/s → 37  $\mu\text{m}$ , substrate velocity o 46.5 m/s → 22  $\mu\text{m}$ ,

- **Operation:** carried out in vacuum, air, or inert atmosphere, or reactive gas depending on the chemical and physical properties of the charge

- **Solidification rate:** typically about  $10^5$ - $10^6$  K/s,

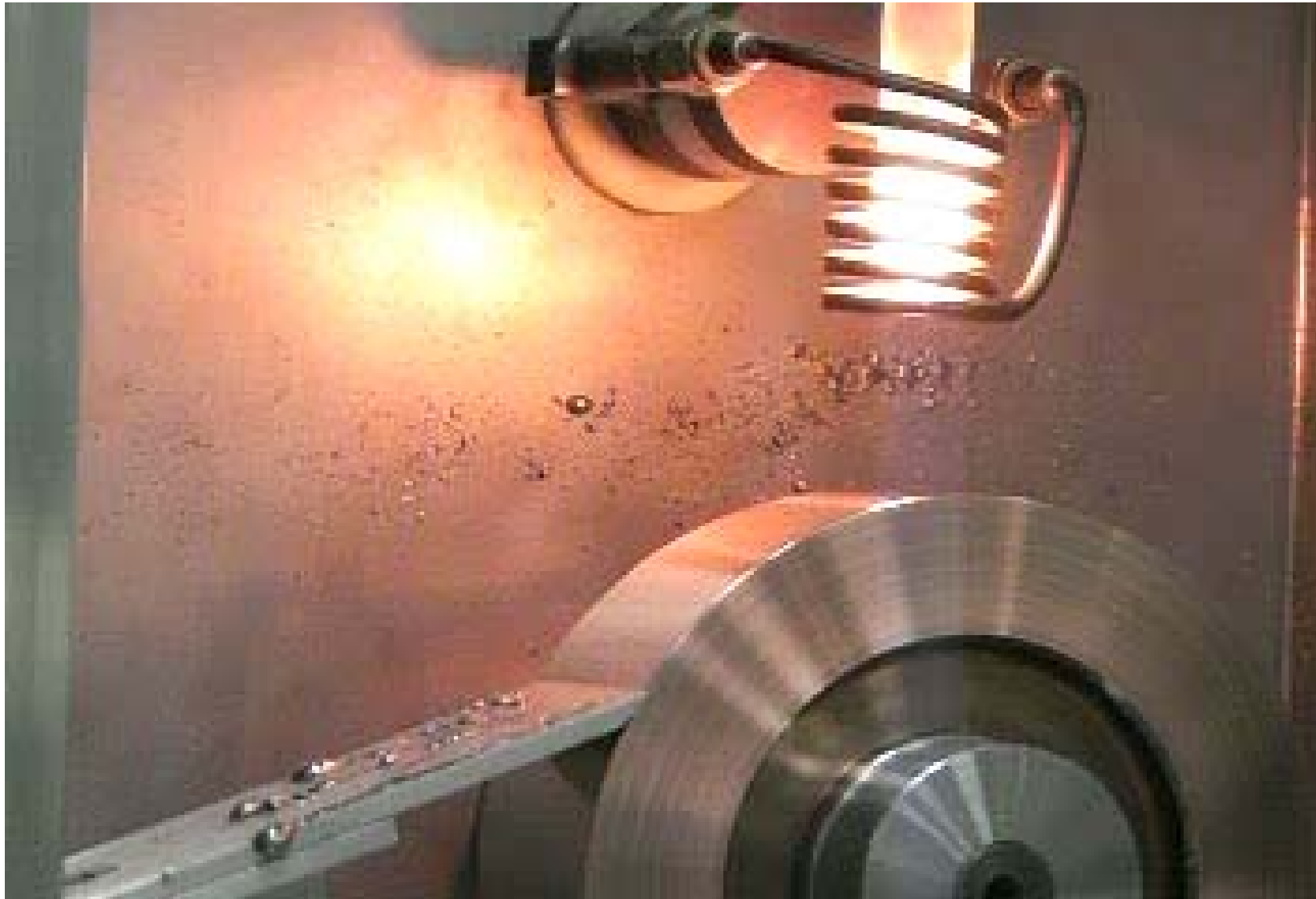
- **Typical dimensions of ribbons:** 2-5 mm → can be increased using the planar flow casting method

- **Thickness:** 20-50  $\mu\text{m}$  → cannot be increased

➡ These thin ribbon used to measure the thermal properties ( $T_g$ ,  $T_x$ , and  $T_l$ ) using the DSC and or DTA methods. This is appropriate because the thermal properties of the glass do not depend on the dimensions of the glass specimen (in general). → **Calculation of GFA parameters**

- **Melt-spinning method**

**Thin film**



## 4.5 Bulk Metallic Glass

### \* History of Metallic Glasses

- First amorphous metal produced by evaporation in 1934.

*\* j. Kramer, Annalen der Phys. 1934; 19: 37.*

- First amorphous alloy (CoP or NiP alloy)  
produced by electro-deposition in 1950.

*\* A. Brenner, D.E. Couch, E.K. Williams, J. Res. Nat. Bur. Stand. 1950: 44; 109.*

- First metallic glass ( $\text{Au}_{80}\text{Si}_{20}$ )  
produced by splat quenching at Caltech by Pol Duwez in 1957.

*\* W. Klement, R.H. Willens, P. Duwez, Nature 1960; 187: 869.*

- First **bulk metallic glass** ( $\text{Pd}_{77.5}\text{Cu}_6\text{Si}_{16.5}$ )  
produced by droplet quenching at Harvard Univ.  
by **H.S. Chen and D. Turnbull** in 1969

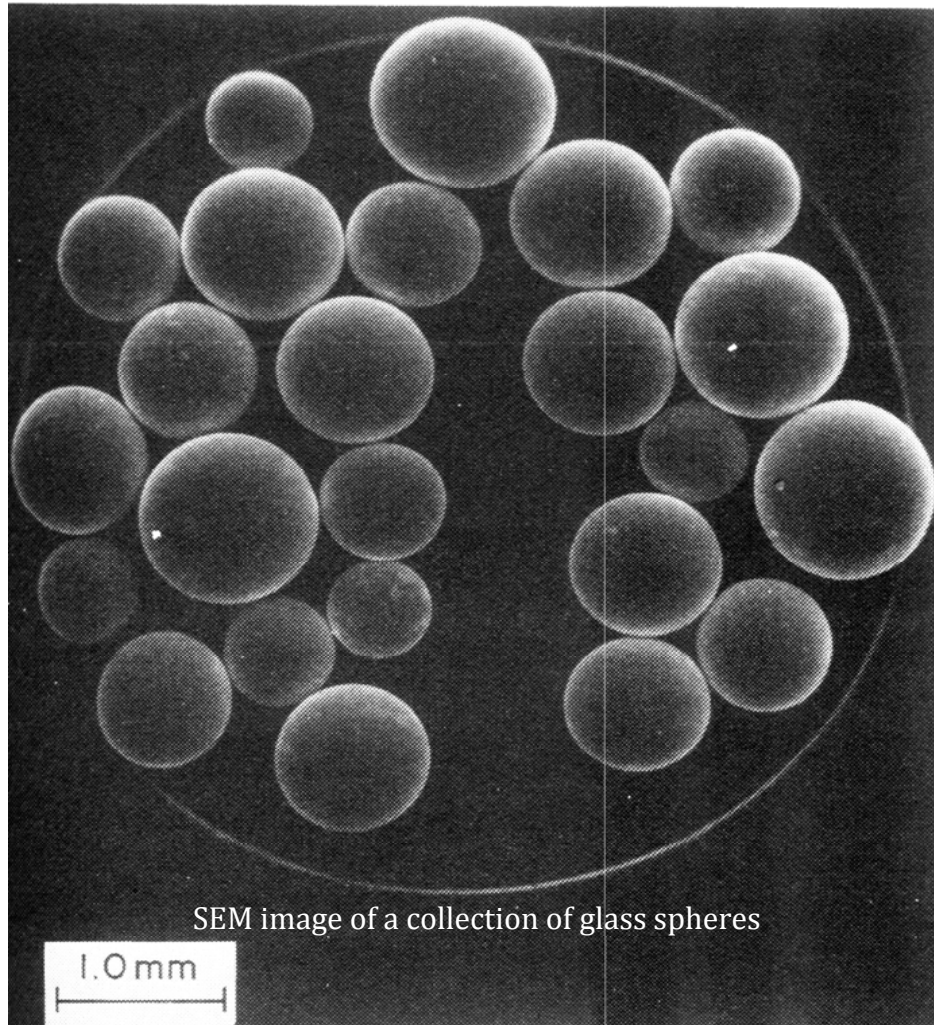
*\* H.S. Chen and D. Turnbull, Acta Metall. 1969; 17: 1021.*

produced by water quenching of PdTMSi, Pt-Ni-P and Pd-Ni-P system  
by **H.S. Chen** in 1974 ( long glassy rods, 1-3 mm in diameter and several centimeters in length)

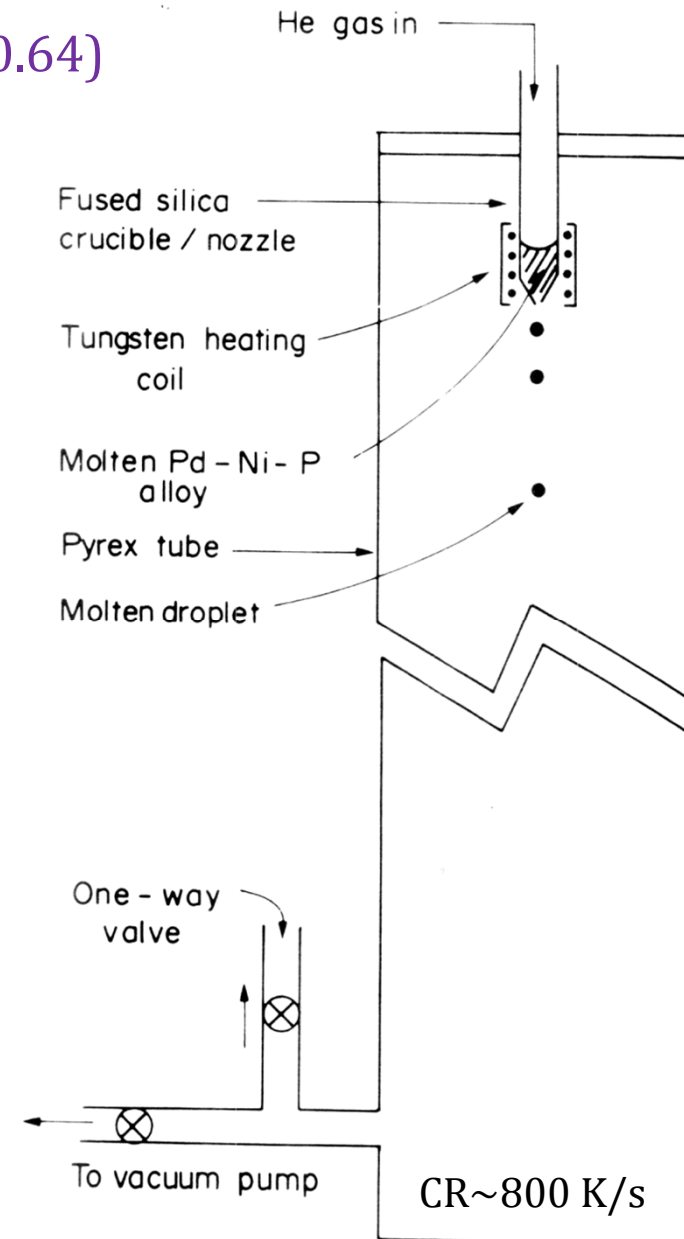
*\* H.S. Chen, Acta Metall. 1974; 22: 1505*

► First bulk metallic glass:  $\text{Pd}_{77.5}\text{Cu}_6\text{Si}_{16.5}$  ( $T_{rg}=0.64$ )

By droplet quenching (CR~800 K/s)



\* H.S. Chen and D. Turnbull, *Acta Metall.* 1969; 17: 1021.



# Bulk formation of a metallic glass: Pd<sub>40</sub>Ni<sub>40</sub>P<sub>20</sub>

## • Suppression of homogeneous nucleation:

Alloy Selection: Consideration of  $T_{rg}$

\* Pd<sub>82</sub>Si<sub>18</sub> →  $T_{rg}=0.6$

- Homogeneous nucleation rate:  $>10^5/\text{cm}^3\text{s}$

- Critical cooling rate:  $> 800 \text{ K/s}$

\* Pd<sub>77.5</sub>Cu<sub>6</sub>Si<sub>16.5</sub> →  $T_{rg}=0.64$

\* Pd<sub>40</sub>Ni<sub>40</sub>P<sub>20</sub> →  $T_{rg}=0.67$

$T_g=590 \text{ K}$ ,  $T_e = 880 \text{ K}$ ,  $T_l = 985 \text{ K}$

## • Suppression of Heterogeneous nucleation: very important in suppressing the nucleation of crystalline phases

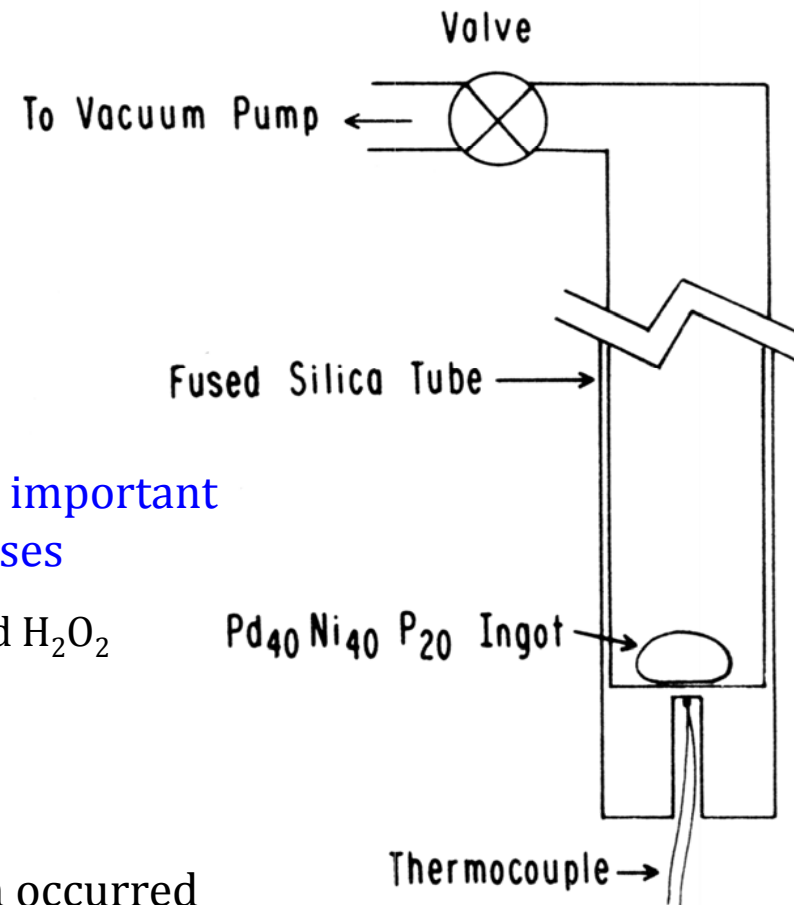
1. Surface Etching of ingot in a mixture of HCL and H<sub>2</sub>O<sub>2</sub>  
: elimination of surface heterogeneities

2. Thermal cycling -5 cycles

: dissolution of nucleating heterogeneities

→ reduce the temperature at which nucleation occurred

<Schematic diagram of apparatus>



# Bulk formation of a metallic glass: Pd<sub>40</sub>Ni<sub>40</sub>P<sub>20</sub>

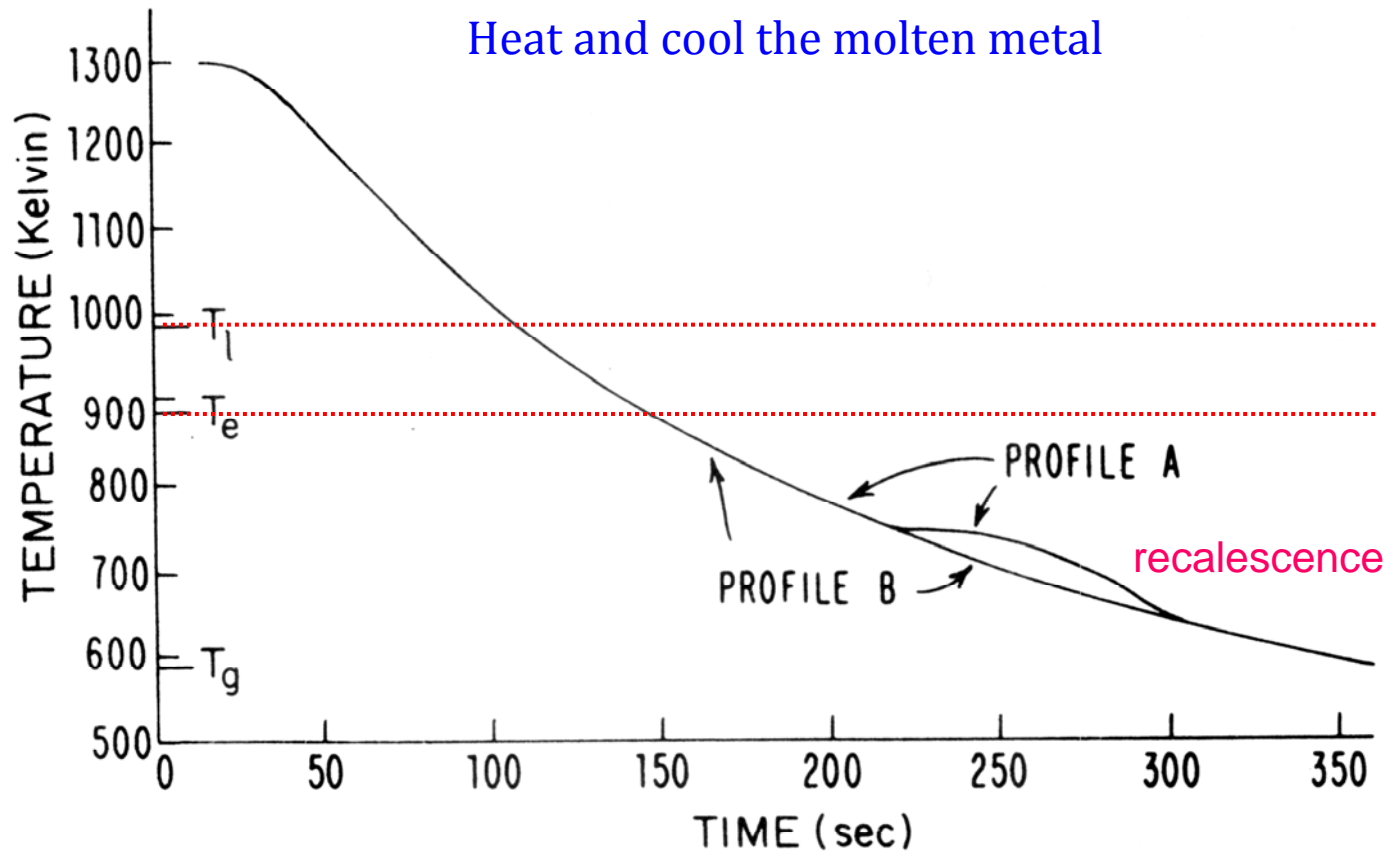


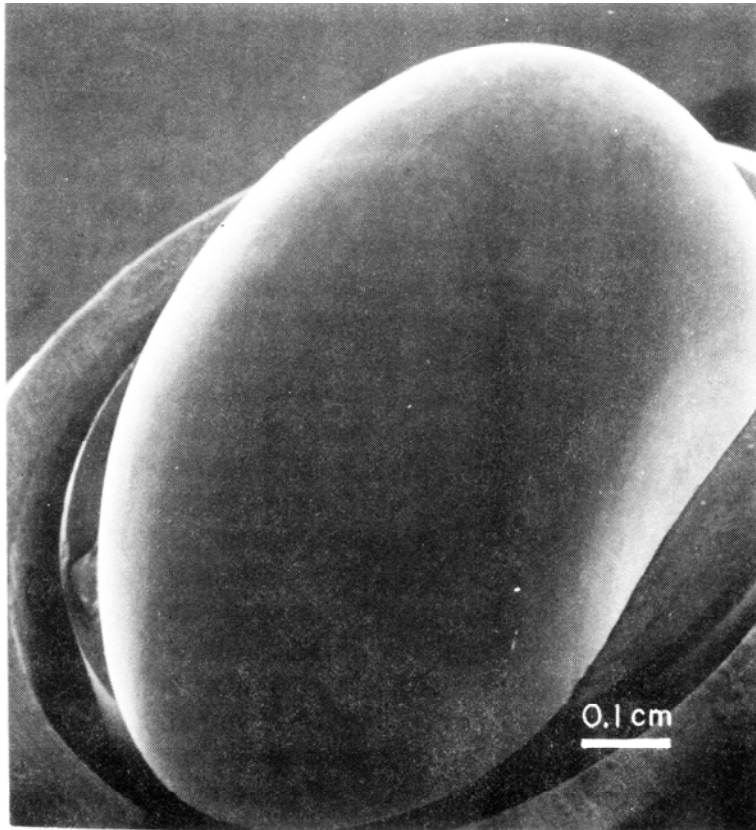
FIG. 2. Superposition of two cooling profiles: A—bulk crystallization which began at 740 K. B—formation of a glassy ingot.

*A.J. Drehman, A.L. Greer, D. Turnbull, Appl. Phys. Lett. 1982; 41: 716.*

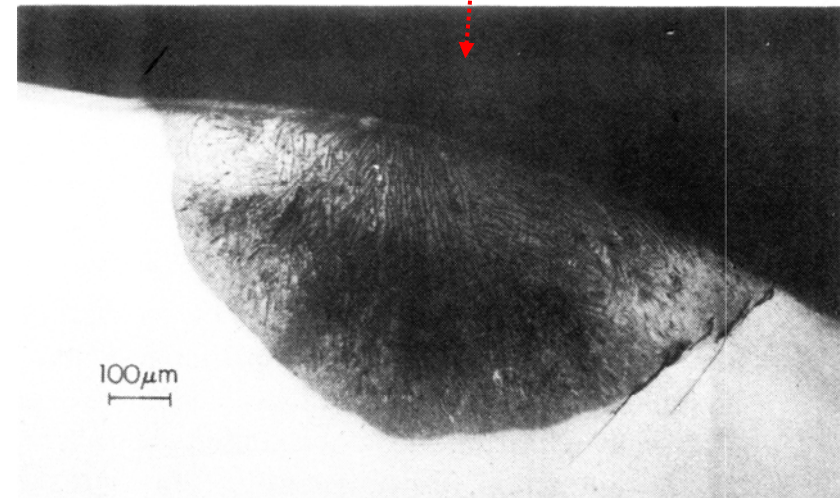
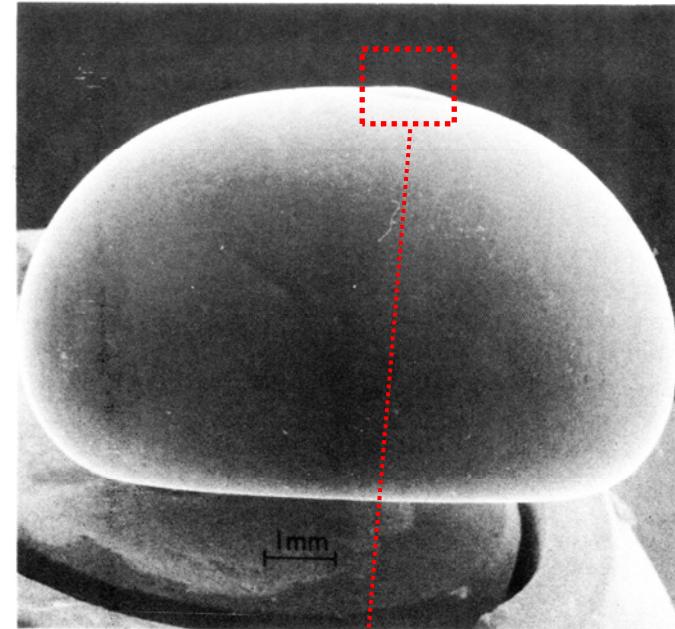
# Bulk formation of a metallic glass: Pd<sub>40</sub>Ni<sub>40</sub>P<sub>20</sub>

- Largest ingot

- minimum dimension 0.6 cm and mass of 2.3 g
- Critical cooling rate: ~ 1.4 K/sec.



*\*Appl. Phys. Lett. 1982; 41: 716.*



OM image of the cross section of a crystalline inclusion showing the eutectic structure

#### 4.5.1 Flux Melting Technique : immersed in molten oxide flux

### Formation of bulk metallic glass by fluxing

#### • Heterogeneous nucleation

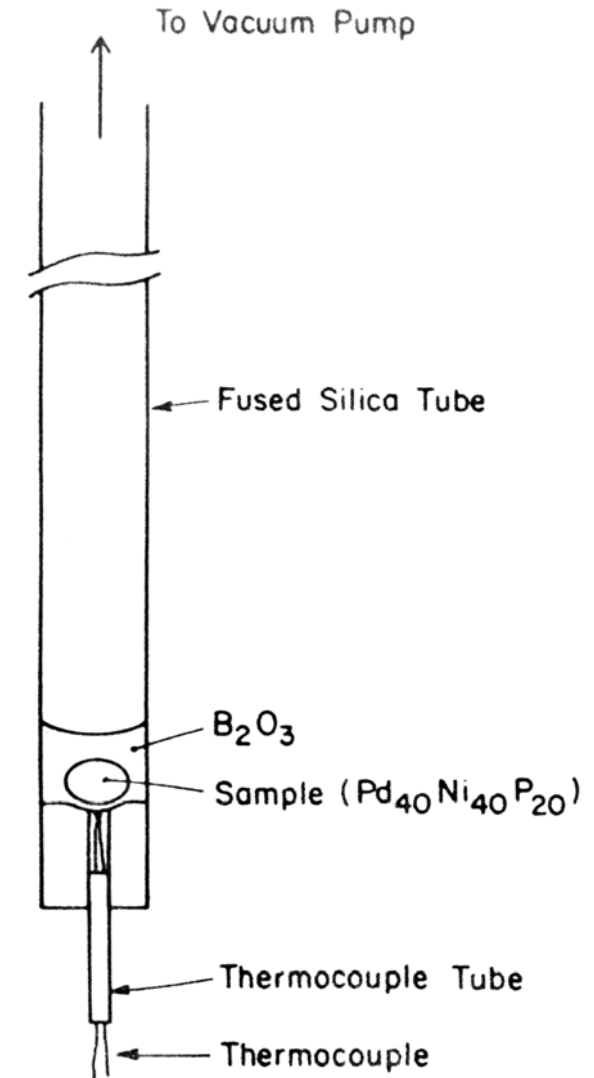
1. Surface oxide layer
2. Container walls
3. Motes in the liquid

#### → Suppression

1. Ingot = Chemical etching  
by dilute aqua regia ( $\text{HNO}_3 + \text{HCl}$ )
2. Interior of the vessel = Cleaning  
by hydrofluoric acid
3. Impurities = Successive heating-cooling cycles  
in a molten oxide flux

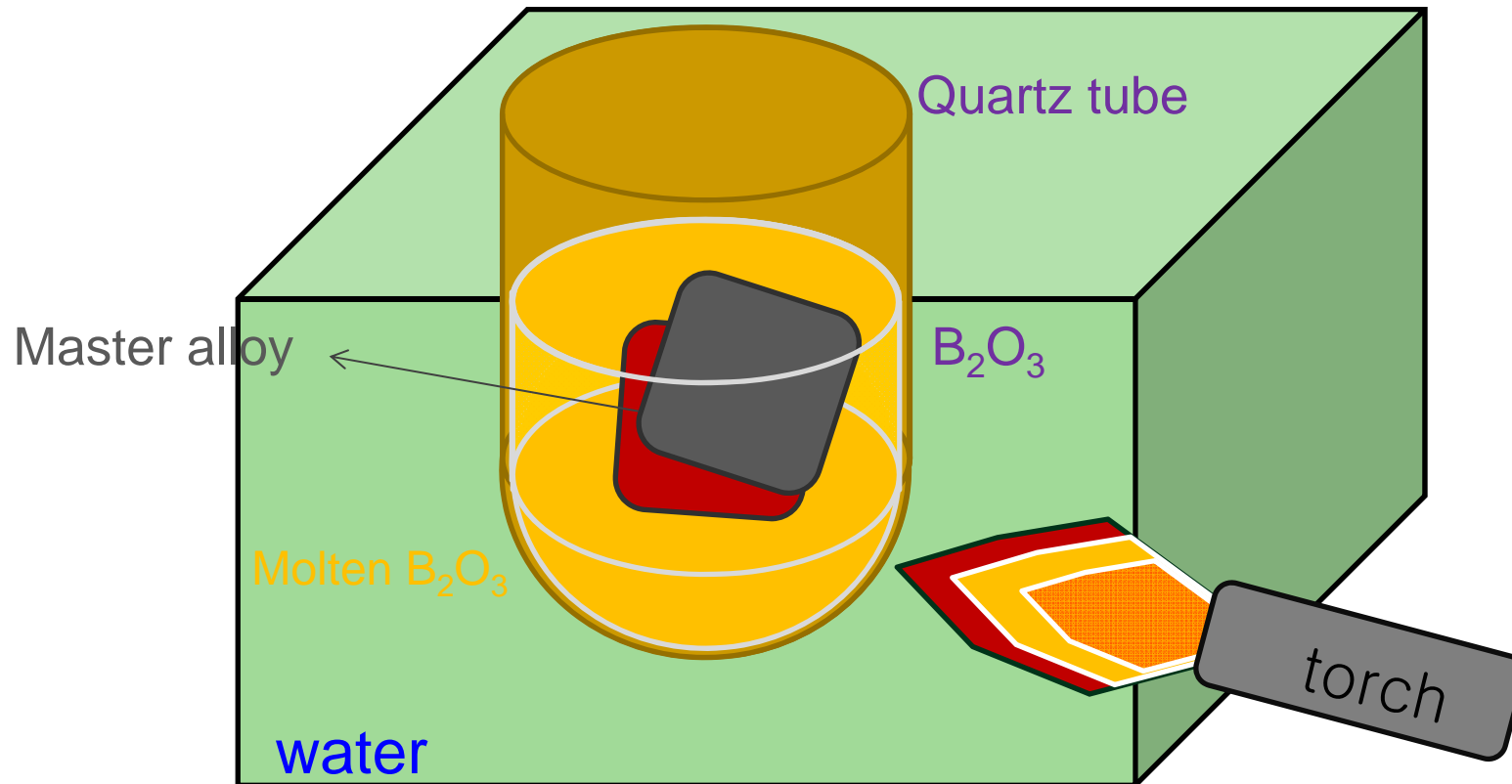
$\text{B}_2\text{O}_3$  melting point 723 K, boiling point  $< 40,000$  K

After gravity segregation to the oxide-metal interface most heterophase impurities presumably are dissolved or deactivated (e.g., by being wet) by the molten oxide (like slag in foundries)



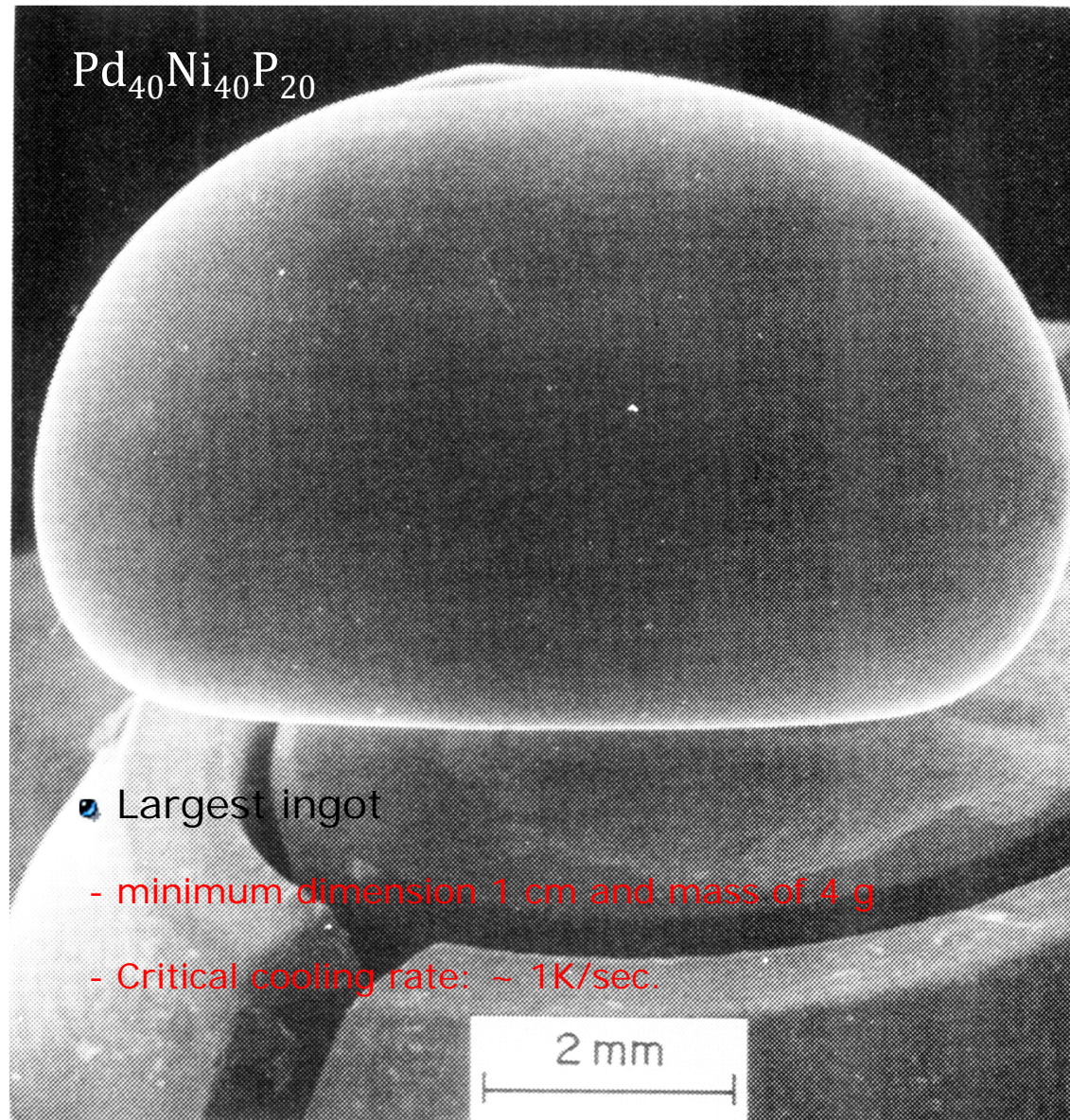
# Schematic process of fluxing

: 1273K → cooling →  $B_2O_3$  still in the molten state at  $T_g$  of  $Pd_{40}Ni_{40}P_{20}$  (600K) ?

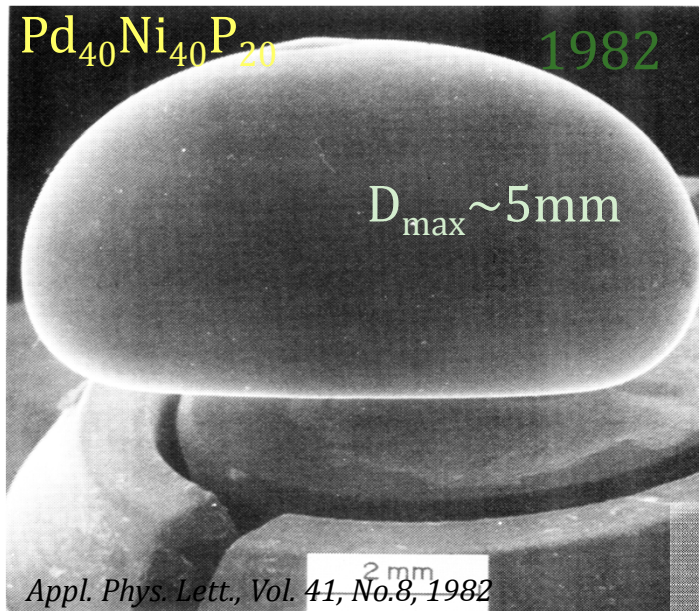


**$B_2O_3$  smelting point 723K (trigonal), Boiling point 2133 K**

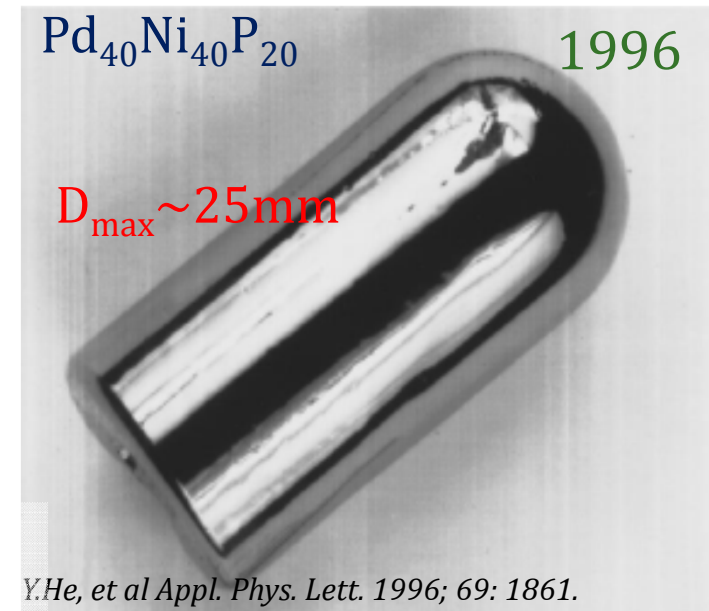
# Formation of centimeter-sized BMG by fluxing



# Formation of centimeter-sized BMG by fluxing



1984  
→  
 $D_{\text{max}} \sim 10\text{mm}$



After  
fluxing  
treatment

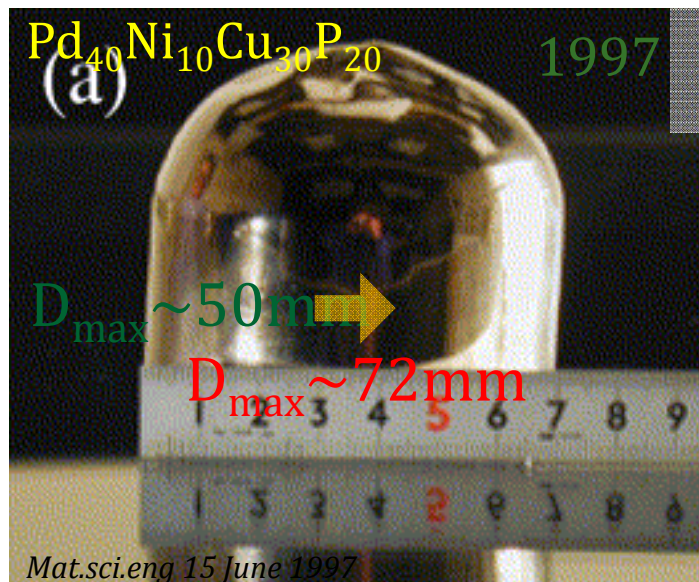


**TABLE 4.1**

Summary of Early Results on Discovery of BMGs

Alloy Composition	Critical Cooling Rate (K s <sup>-1</sup> )	Year of Discovery	Largest Section Thickness (mm)	Reference
(Pd <sub>1-x</sub> M <sub>x</sub> ) <sub>0.835</sub> Si <sub>0.165</sub> (M = Cu, Ag, Au, Fe, Co, Ni)	—	1974	1–3	[18]
(Pd <sub>1-x</sub> T <sub>x</sub> ) <sub>1-xP</sub> P <sub>xP</sub> or (Pt <sub>1-x</sub> T <sub>x</sub> ) <sub>1-xP</sub> P <sub>xP</sub> (T = Fe, Co, or Ni)	—	1974	1–3	[18]
Pd <sub>40</sub> Ni <sub>40</sub> P <sub>20</sub>	1	1982	5	[20]
Pd <sub>40</sub> Ni <sub>40</sub> P <sub>20</sub> (flux treated)	—	1984	10	[21]
La <sub>55</sub> Al <sub>25</sub> Ni <sub>20</sub>	—	1989	1.2	[23]
Mg <sub>65</sub> Cu <sub>25</sub> Y <sub>10</sub>	—	1992	7	[24]
Zr <sub>41.2</sub> Ti <sub>13.8</sub> Cu <sub>12.5</sub> Ni <sub>10</sub> Be <sub>22.5</sub>	~1	1993	14	[25]
Pd <sub>40</sub> Ni <sub>10</sub> Cu <sub>30</sub> P <sub>20</sub>	1.57	1996	40	[26]
Pd <sub>40</sub> Ni <sub>10</sub> Cu <sub>30</sub> P <sub>20</sub> (flux treated)	0.1	1997	72	[19]

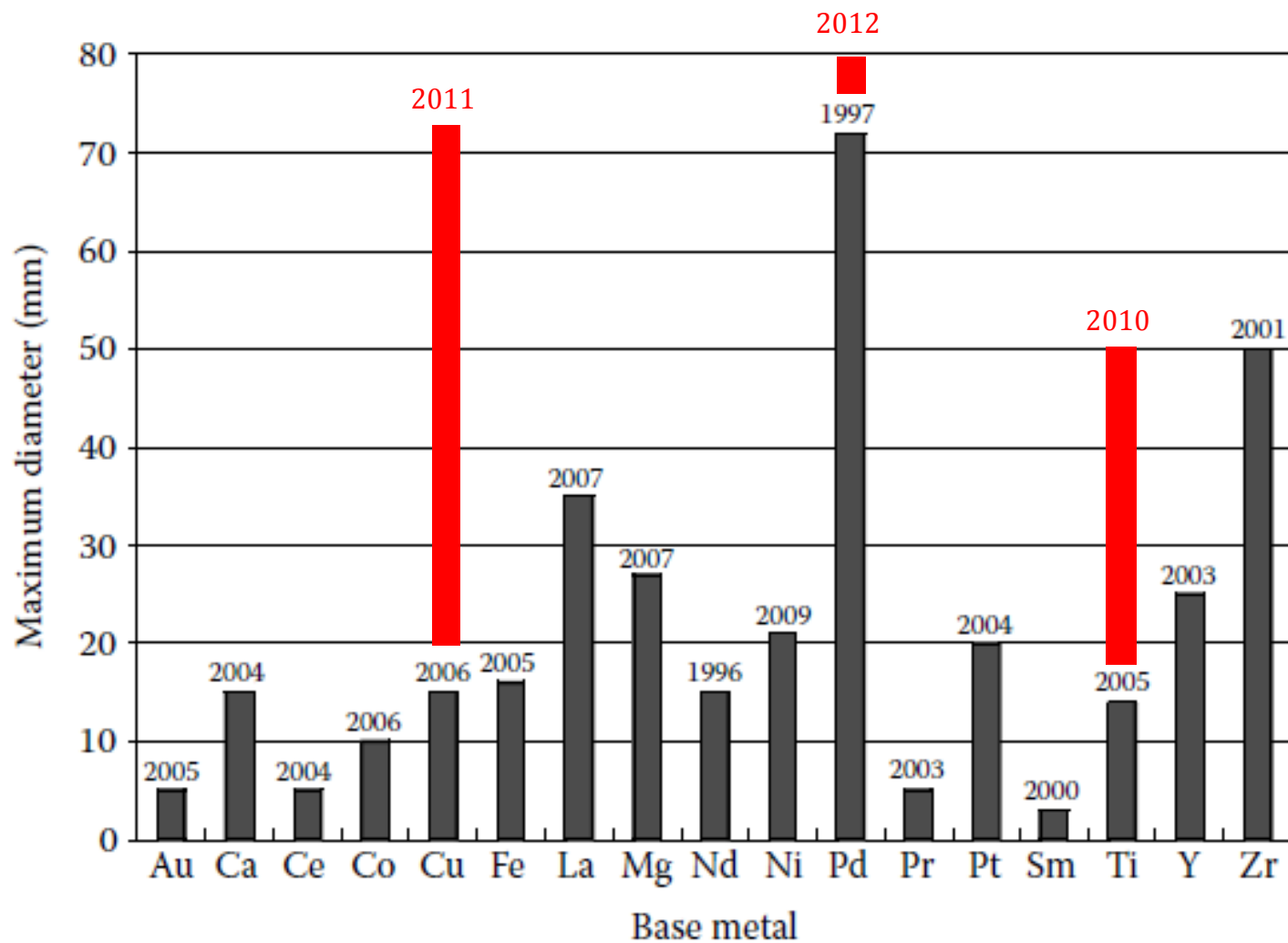


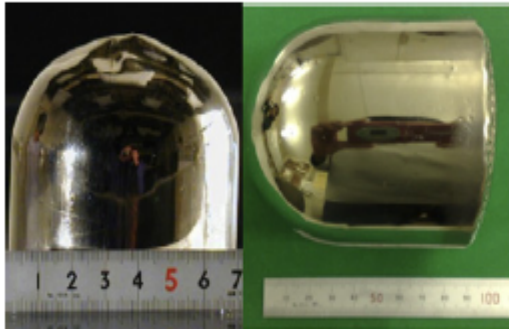
**FIGURE 2.7**

Maximum diameters of the BMG rods achieved in different alloy systems and the years in which they were discovered.

# Bulk glass formation in the Pd-/Ni-/Cu-/Zr- element system

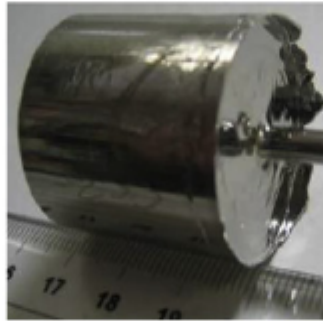
## Massy Ingot Shape

(a) Pd-Cu-Ni-P



72φx 75 mm 80φx 85 mm

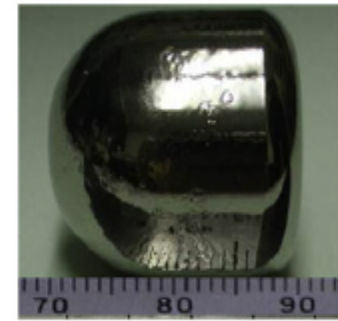
(b) Zr-Al-Ni-Cu



(c) Cu-Zr-Al-Ag

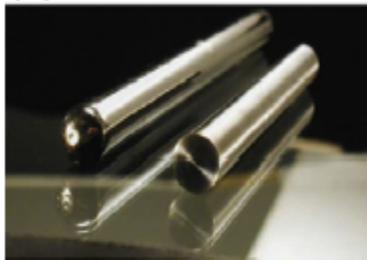


(d) Ni-Pd-P-B

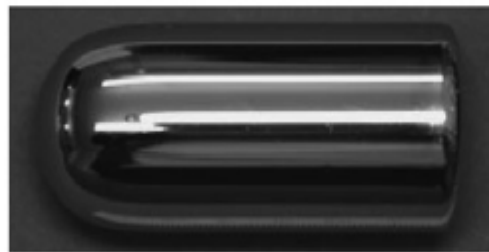


## Cylindrical Rods

(e) Pd-Cu-Ni-P

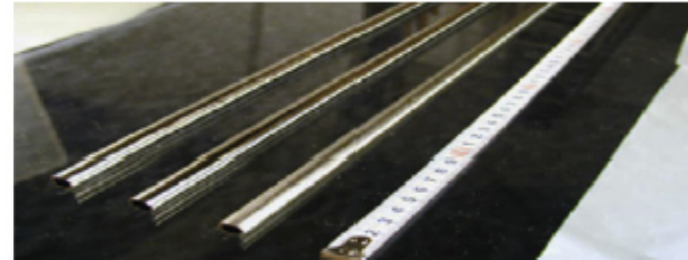


(f) Pt-Pd-Cu-P



## Hollow Pipes

(g) Pd-Cu-Ni-P



## 4.5.2 Role of Contamination

Zirconium and Titanium based BMG: very sensitive to the presence of impurities

- Ex) - high oxygen contents reduced the supercooled liquid region and changed the crystallization behavior (formation of quasicrystals) in Zr based BMGs.  
- it is possible that other interstitial elements may also have a significant effect like O.

1) Crystallization incubation time decreased by orders of magnitude as one went from 250 to 5250 ppm of oxygen (oxygen content  $\uparrow$   $\rightarrow$  incubation time  $\downarrow$ )

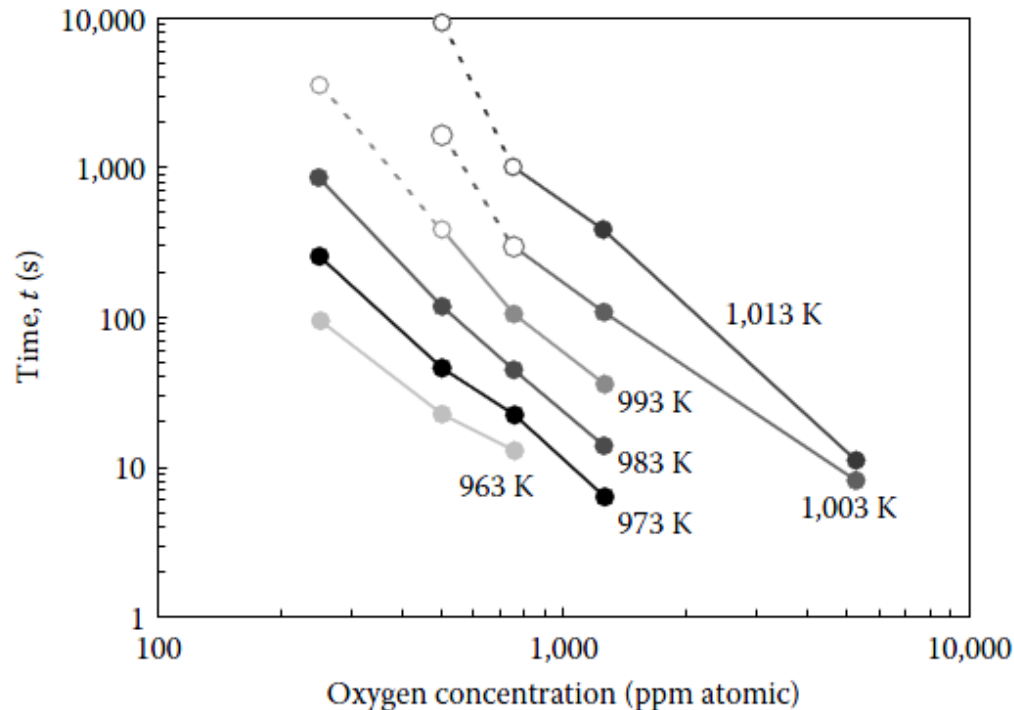


FIGURE 4.2

Crystallization incubation time at different temperatures as a function of oxygen content in a  $Zr_{52.5}Ti_5Cu_{17.9}Ni_{14.6}Al_{10}$  bulk glassy alloy. (Reprinted from Lin, X.H. et al., *Mater. Trans., JIM*, 38, 473, 1997. With permission.)

# Effect of Oxygen Impurity on Crystallization of an Undercooled Bulk Glass Forming Zr-Ti-Cu-Ni-Al Alloy

X. H. Lin\*, W. L. Johnson\* and W. K. Rhim\*\*

\*W. M. Keck Laboratory of Engineering Materials, California Institute of Technology, Pasadena, CA 91125, USA

\*\*Jet Propulsion Laboratory, California Institute of Technology, Pasadena, CA 91109, USA

High vacuum, containerless, electrostatic levitation process has been used to study the undercooling and crystallization kinetics of a bulk glass forming Zr-Ti-Cu-Ni-Al alloy. The oxygen impurity level in the alloy has been found to play a crucial role in the crystallization kinetics of the undercooled melt.

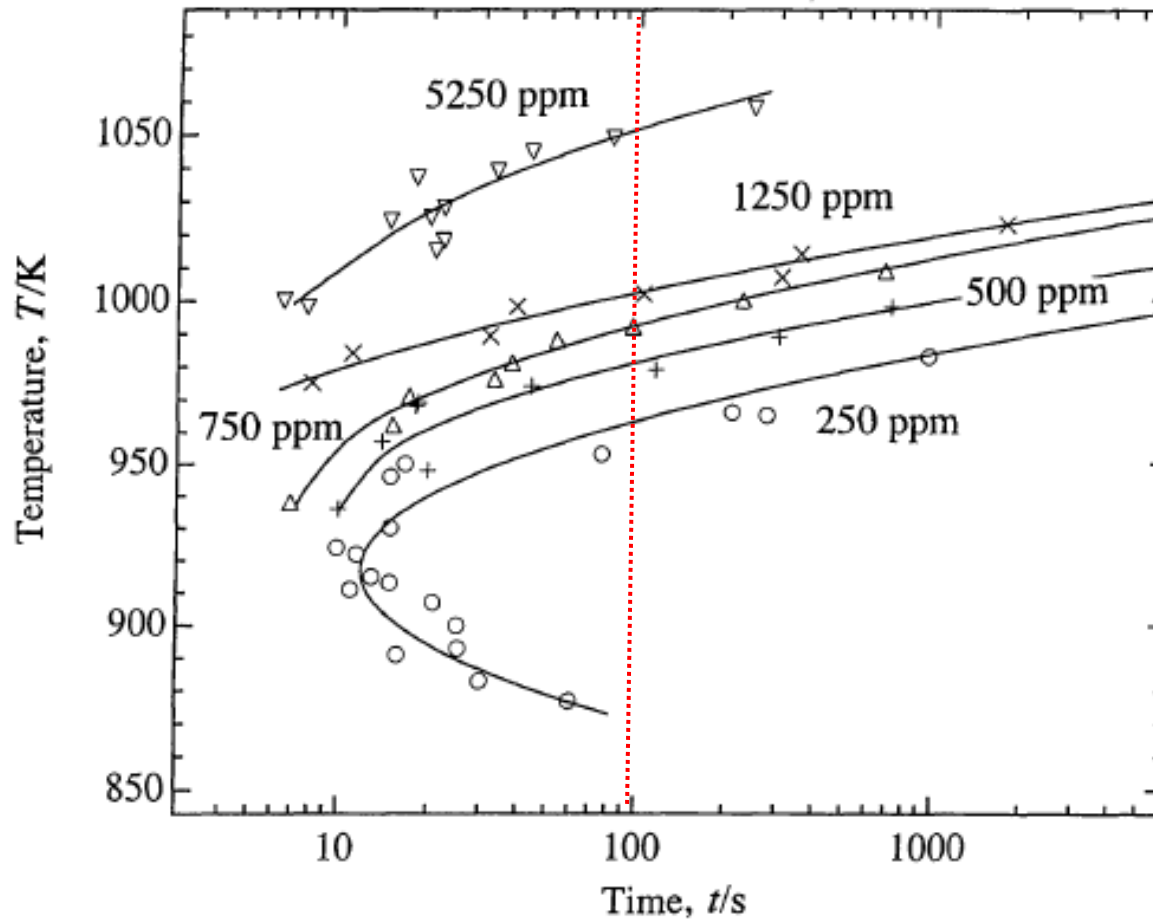


Fig. 5 Time-temperature-transformation diagrams of alloys of 5250, 1250, 750, 500 and 250 atom ppm oxygen respectively.

- 2) Effect of oxygen content (0.28-0.6 at.%) on the thermal stability of the glassy phase  
 : GFA decreased with increasing oxygen content. (oxygen content  $\uparrow \rightarrow T_g \uparrow$  &  $T_x \downarrow$ )  
 $\rightarrow$  need to be careful in directly correlating the extent of SLR with the high GFA of alloys especially in reactive alloy system such as those based on Zirconium or Titanium

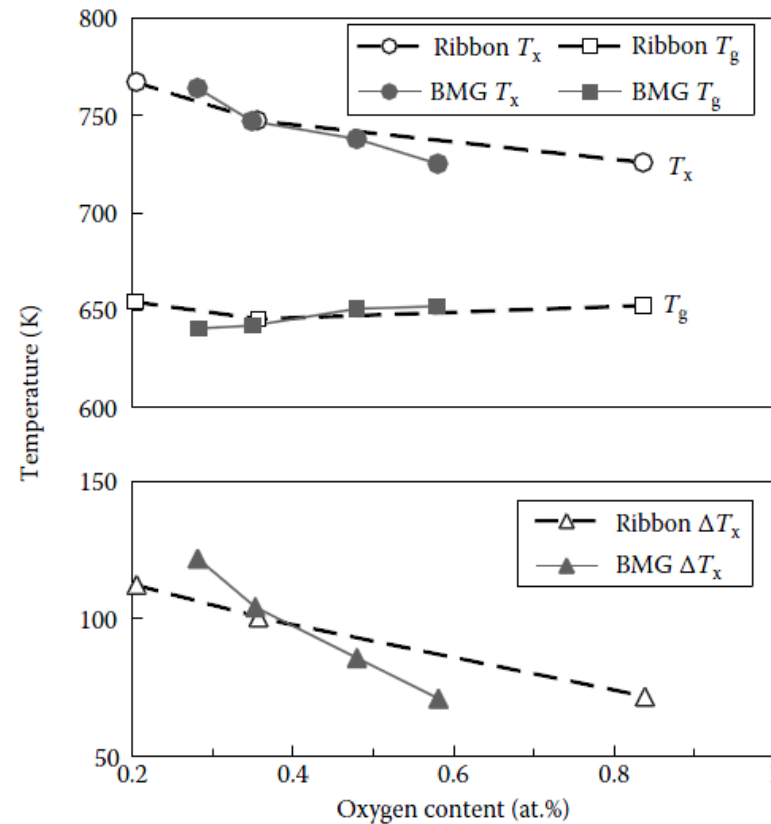


FIGURE 4.3  
 Variation of  $T_g$ ,  $T_x$ , and  $\Delta T_x$  as a function of the oxygen content in the Zr-glassy alloys. Results for both bulk samples and melt-spun ribbons are shown. (Reprinted from Gebert, A. et al., *Acta Mater.*, 46, 5475, 1998. With permission.)

**➡ Scavenger effect:** addition of strong oxide-forming elements  $\rightarrow$  reduce oxygen content  $\rightarrow$  GFA  $\uparrow$

ex)  $Zr_{52.5}Cu_{17.9}Ni_{14.6}Al_{10}Ti_5$  with 0.03-0.06 at.%Sc  $\rightarrow$   $Sc_2O_3 \uparrow \rightarrow$  GFA  $\uparrow$  up to 12mm

## 4.6 Bulk Metallic Glass Casting Methods

**4.6.1 Water-Quenching Method** : simplest of the quenching methods used for centuries to harden steel (by transforming the soft austenite to the hard martensite phase)

- **Cooling rate: about 10-100 K/s**, inherently dependent on the heat transfer efficiency of quenching medium, the size of the specimen, and its heat transfer properties.
- A distinct advantage of the water-quenching method is that due to the slow solidification rates, the cast specimen **contains much less residual stresses and porosity**.

The world's biggest glassy alloy ever made

*Intermetallics* 30 (2012) 19–24

Nobuyuki Nishiyama<sup>a,\*</sup>, Kana Takenaka<sup>a</sup>, Haruko Miura<sup>a</sup>, Noriko Saidoh<sup>a</sup>, Yuqiao Zeng<sup>b</sup>, Akihisa Inoue<sup>b</sup>

<sup>a</sup>RIMCOF Tohoku Univ. Lab., The Materials Process Technology Center, Sendai 980-8577, Japan

<sup>b</sup>Institute for Materials Research, Tohoku University, Sendai 980-8577, Japan

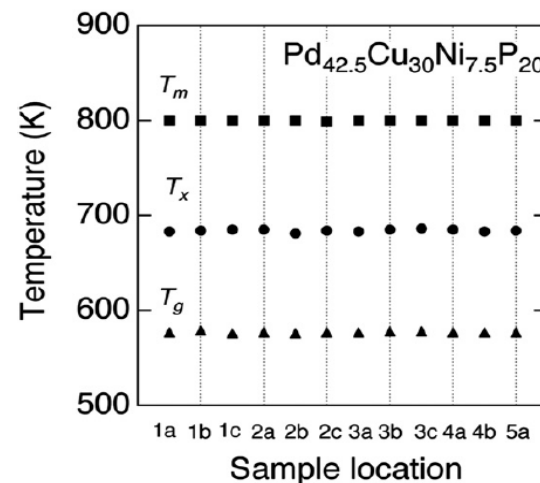
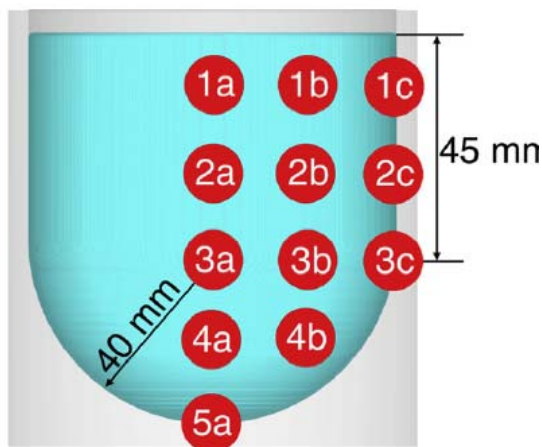


**TABLE 4.2**

Details of Bulk Metallic Glassy Rods Produced by the Water Quenching Method

Alloy System	Diameter of the Rod (mm)	Critical Cooling Rate (K s <sup>-1</sup> )	Year	Reference
(Pd <sub>1-x</sub> M <sub>x</sub> ) <sub>0.835</sub> Si <sub>0.165</sub>	1–3	<10 <sup>3</sup>	1974	[18]
(Pd <sub>1-x</sub> Ti <sub>x</sub> ) <sub>1-x</sub> P <sub>x</sub> P	1–3	<10 <sup>3</sup>	1974	[18]
(Pt <sub>1-x</sub> Ni <sub>x</sub> ) <sub>1-x</sub> P <sub>x</sub> P	1–3	<10 <sup>3</sup>	1974	[18]
Pd <sub>40</sub> Ni <sub>40</sub> P <sub>20</sub>	5–6	~1	1982	[20]
Pd <sub>40</sub> Ni <sub>40</sub> P <sub>20</sub> (flux treated)	10		1984	[21]
Zr <sub>65</sub> Al <sub>7.5</sub> Ni <sub>10</sub> Cu <sub>17.5</sub>	<16	1.5	1993	[37]
Zr <sub>41.2</sub> Ti <sub>13.8</sub> Cu <sub>12.5</sub> Ni <sub>10</sub> Be <sub>22.5</sub>	14	<10	1993	[25]
Pd <sub>40</sub> Cu <sub>30</sub> Ni <sub>10</sub> P <sub>20</sub>	40	1.57	1996	[26]
Pd <sub>40</sub> Cu <sub>30</sub> Ni <sub>10</sub> P <sub>20</sub> (flux treated)	50–72	0.1	1997	[19]
Pd <sub>40</sub> Ni <sub>40</sub> P <sub>20</sub>	7	100	1999	[38]
Pd <sub>40</sub> Ni <sub>32.5</sub> Fe <sub>7.5</sub> P <sub>20</sub>	7	100	1999	[38]
Pd <sub>40</sub> Ni <sub>20</sub> Fe <sub>20</sub> P <sub>20</sub>	7	100	1999	[38]
Mg <sub>65</sub> Y <sub>10</sub> Cu <sub>15</sub> Ag <sub>5</sub> Pd <sub>5</sub>	12		2001	[39]
Y <sub>56</sub> Al <sub>24</sub> Co <sub>20</sub>	1.5		2003	[40]
Y <sub>36</sub> Sc <sub>20</sub> Al <sub>24</sub> Co <sub>20</sub>	25		2003	[40]
Pt <sub>60</sub> Cu <sub>20</sub> P <sub>20</sub>	<4		2004	[41]
Pt <sub>60</sub> Cu <sub>16</sub> Co <sub>2</sub> P <sub>22</sub> (flux treated)	16		2004	[41]
Pt <sub>57.5</sub> Cu <sub>14.7</sub> Ni <sub>5.3</sub> P <sub>22.5</sub> (flux treated)	16		2004	[41]
Pt <sub>42.5</sub> Cu <sub>27</sub> Ni <sub>9.5</sub> P <sub>21</sub> (flux treated)	20		2004	[41]

Most common container material: Quartz but compatibility between melt and the crucible \_important issue For MG BMG, when a quartz tube was used, Si dissolved in the Mg melt as an impurity and acted as heterogeneous nucleation sites. Consequently, the GFA of the alloy was reduced. On the other hand, when an iron tube was used, there was no interaction between iron and the Mg-melt. → D<sub>max</sub> = 12 mm

## 4.6 Bulk Metallic Glass Casting Methods

### 4.6.2 High-Pressure Die Casting

: offer high solidification rates (because heat is extracted more rapidly by the metal mold due to good contact), high productivity, low casting defect, and possible to produce more complex shapes even in alloys with a high viscosity

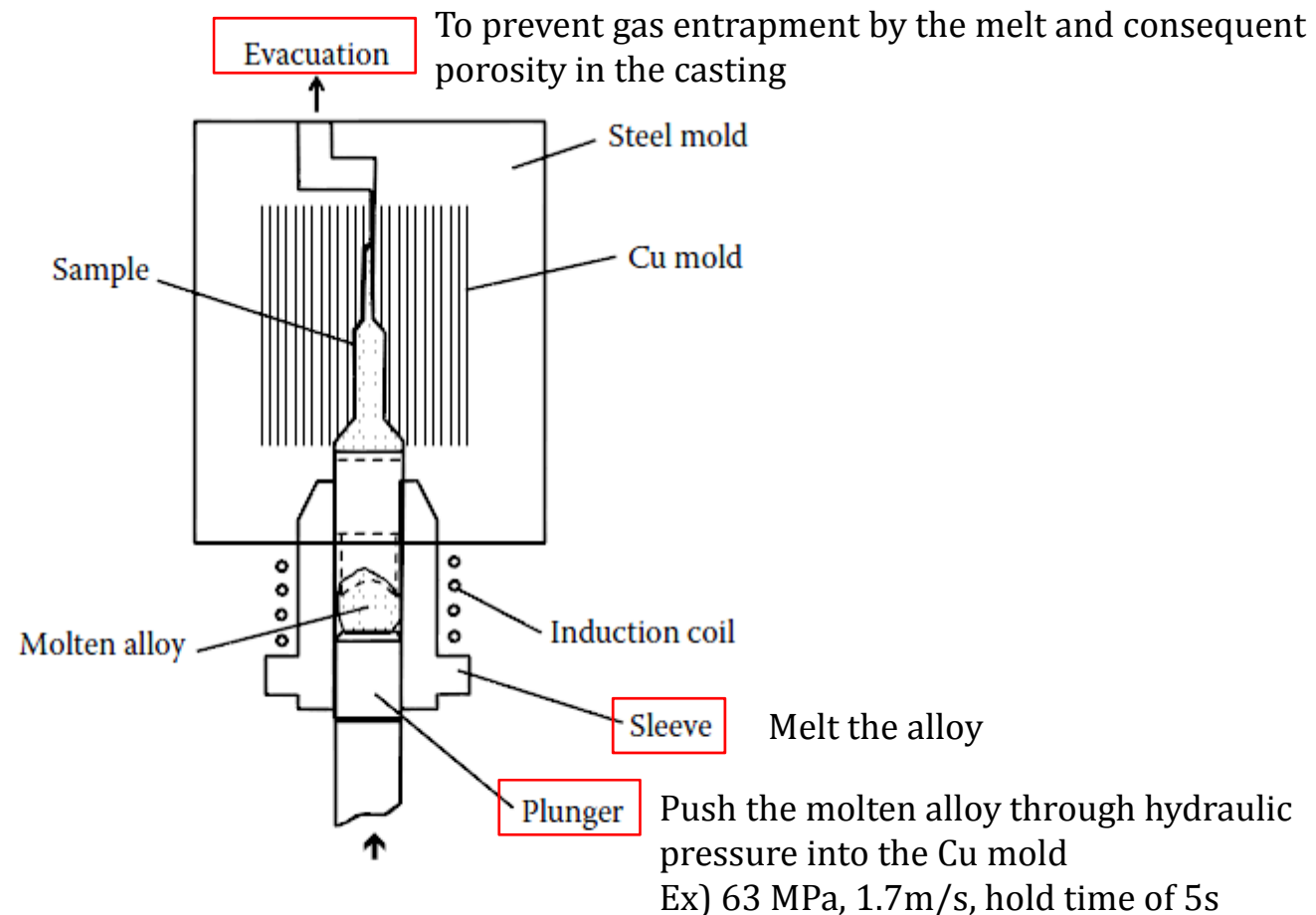
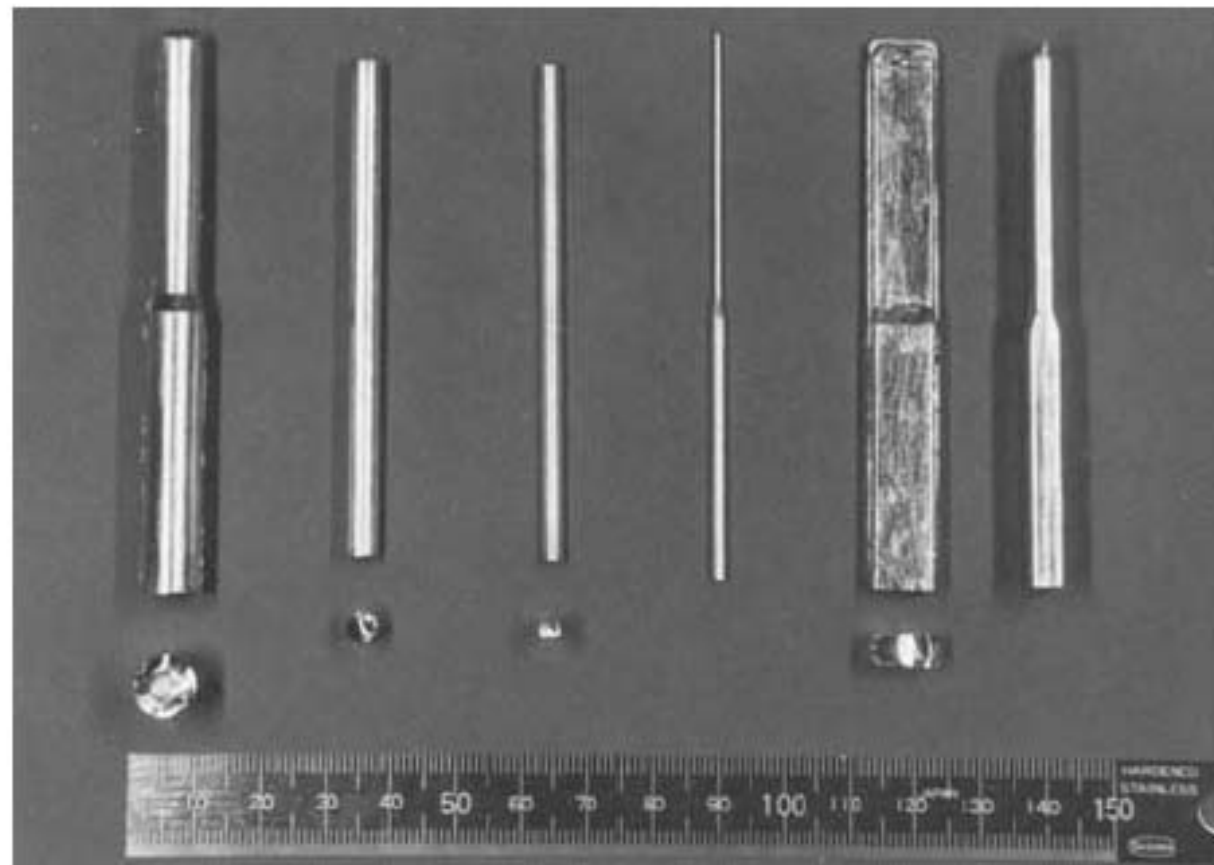


FIGURE 4.5

Schematic diagram of the high-pressure die casting equipment designed and used by Inoue et al. (Reprinted from Inoue, A. et al., *Mater. Trans., JIM*, 33, 937, 1992. With permission.)



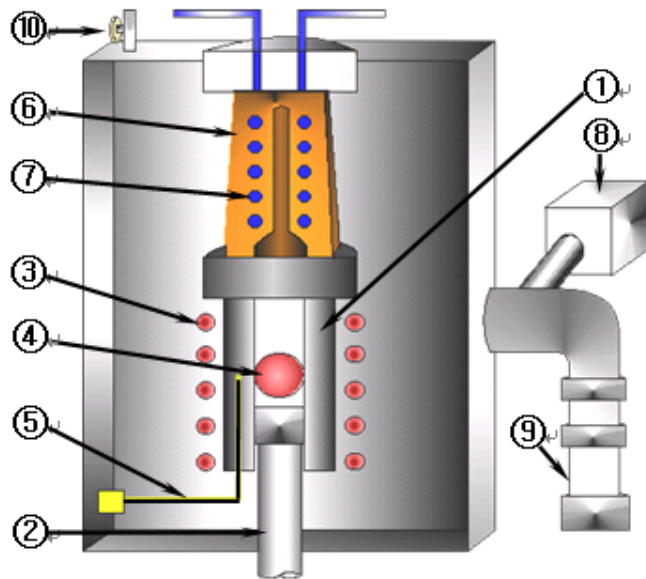
**FIGURE 4.6**

Photographs of the  $\text{Mg}_{65}\text{Cu}_{25}\text{Y}_{10}$  rods and sheets (of different diameters) produced by the high-pressure die-casting technique. The length of the samples is 80 mm and the thickness or diameter varies from 0.5 to 9 mm. Note the bright and shiny appearance of both the types of samples. (Reprinted from Inoue, A. et al., *Mater. Trans., JIM*, 33, 937, 1992. With permission.)

## 4.6 Bulk Metallic Glass Casting Methods

### 4.6.6 Squeeze-casting Method

: involves solidification of the molten metal under a high pressure within a closed die by utilizing a hydraulic pressure → Net-shape forming capability, fully dense sample



①	Graphite crucible	⑥	Copper mold
②	Plunger	⑦	Water cooling
③	Induction coil	⑧	Rotary pump
④	Molten alloy	⑨	Diffusion pump
⑤	Thermocouple	⑩	Evacuation valve

Squeeze Casting  
10mm



Push the molten alloy through hydraulic pressure into the Cu mold  
Ex) 100 MPa, hold time of 2min until the liquid alloy completely solidified

→ Undercooling to much below the equilibrium solidification temperature

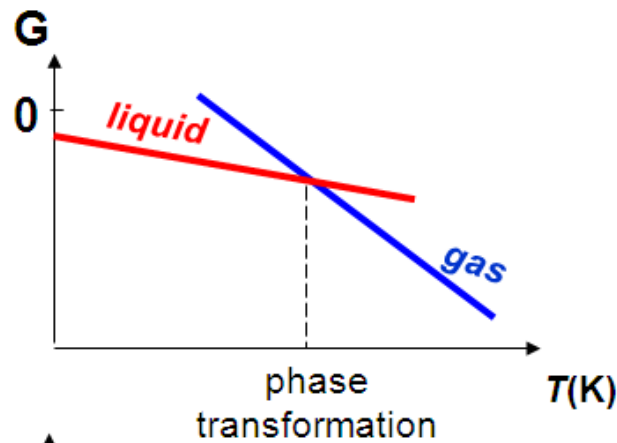
# Gibbs Free Energy as a Function of Temp. or Pressure

Considering P, T  $G = G(T, P)$

$$dG = VdP - SdT$$

$$G(P, T) = G(P_0, T_0) + \int_{P_0}^{P_1} V(T_0, P)dP - \int_{T_0}^{T_1} S(P, T)dT$$

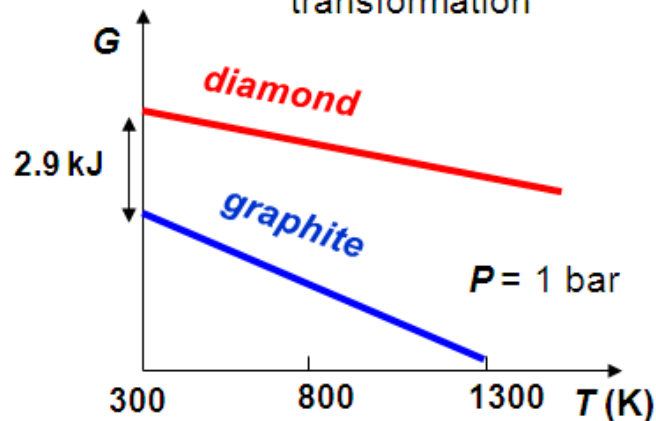
## 1) Temperature Effects



$$S(\text{water}) = 70 \text{ J/K}$$

$$S(\text{vapor}) = 189 \text{ J/K}$$

$$\left(\frac{\partial G}{\partial T}\right)_P = -S$$



$$S(\text{graphite}) = 5.74 \text{ J/K,}$$

$$S(\text{diamond}) = 2.38 \text{ J/K,}$$

**2) Pressure Effects** Different molar volume 을 가진 두 상이 평형을 이룰 때 만일 압력이 변한다면 평형온도 T 또한 압력에 따라 변해야 한다.

If  $\alpha, \beta$  phases are equilibrium,

$$dG^\alpha = V^\alpha dP - S^\alpha dT \quad \left(\frac{dP}{dT}\right)_{eq} = \frac{S^\beta - S^\alpha}{V^\beta - V^\alpha} = \frac{\Delta S}{\Delta V}$$

$$dG^\beta = V^\beta dP - S^\beta dT \quad \text{where, } \Delta S = \frac{\Delta H}{T_{eq}}$$

At equilibrium,

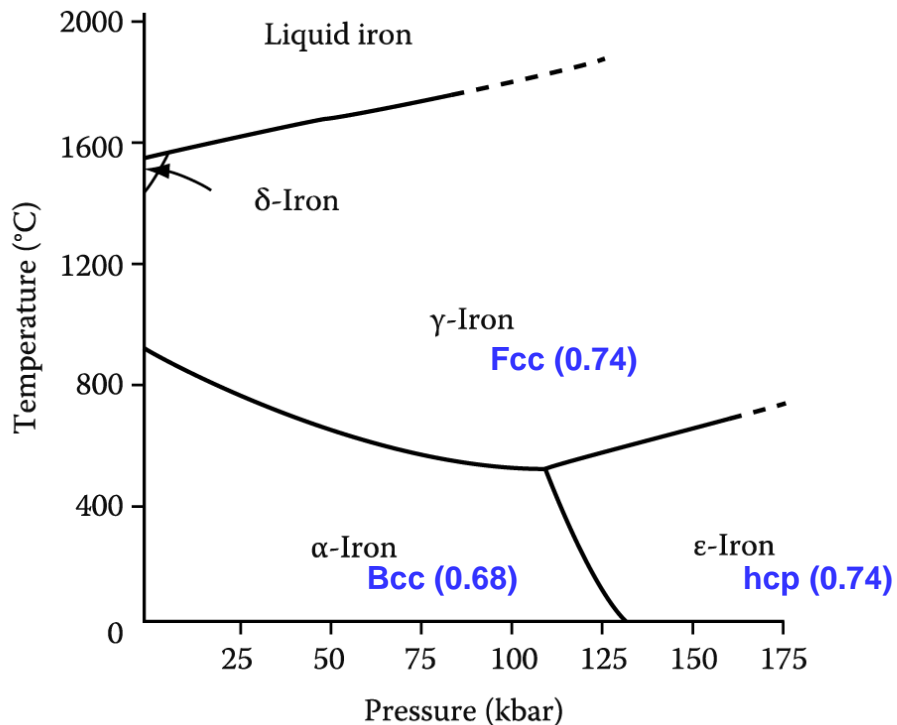
$$dG^\alpha = dG^\beta$$

$$\left(\frac{dP}{dT}\right)_{eq} = \frac{\Delta H}{T_{eq} \Delta V}$$

**: Clausius-Clapeyron Relation**

(applies to all coexistence curves)

On a pressure-temperature (P-T) diagram, the line separating the two phases is known as the coexistence curve. The Clausius-Clapeyron relation gives the slope of this curve.



**Case 1.  $\gamma \rightarrow$ liquid ;  $\Delta V (+)$ ,  $\Delta H(+)$**

$$\left(\frac{dP}{dT}\right) = \frac{\Delta H}{T_{eq} \Delta V} > 0$$

**Case 2.  $\alpha \rightarrow \gamma$  ;  $\Delta V (-)$ ,  $\Delta H(+)$**

$$\left(\frac{dP}{dT}\right) = \frac{\Delta H}{T_{eq} \Delta V} < 0$$

Fig. 1.5 Effect of pressure on the equilibrium phase diagram for pure iron

## 4.6 Bulk Metallic Glass Casting Methods

### 4.6.3 Copper Mold Casting

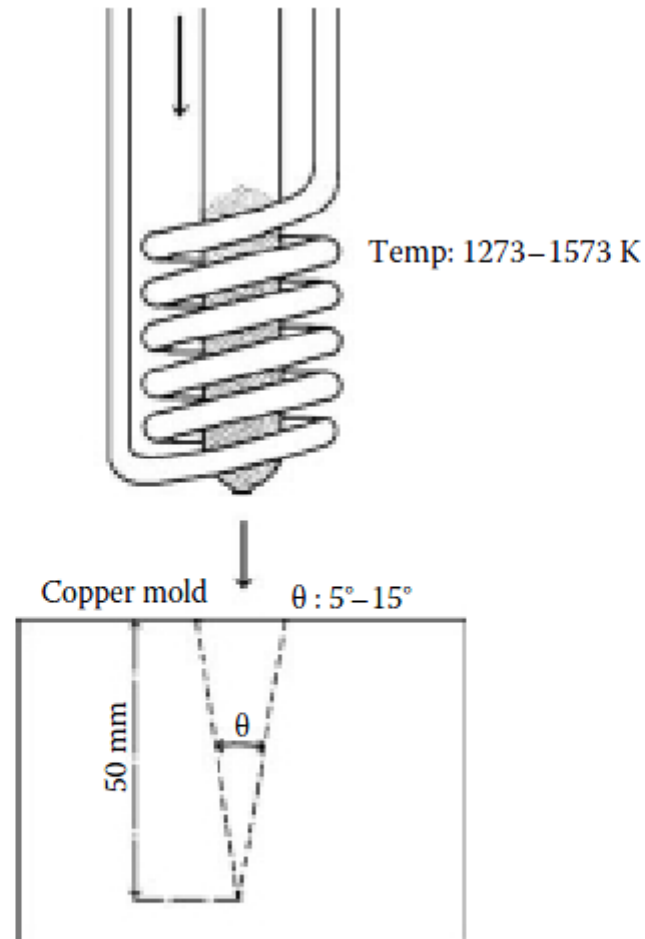


**FIGURE 4.7**

Schematic diagram of the equipment used to prepare bulk metallic glassy alloys by the copper mold wedge-casting technique. (Reprinted from Inoue, A. et al., *Mater. Trans., JIM*, 36, 1276, 1995. With permission.)

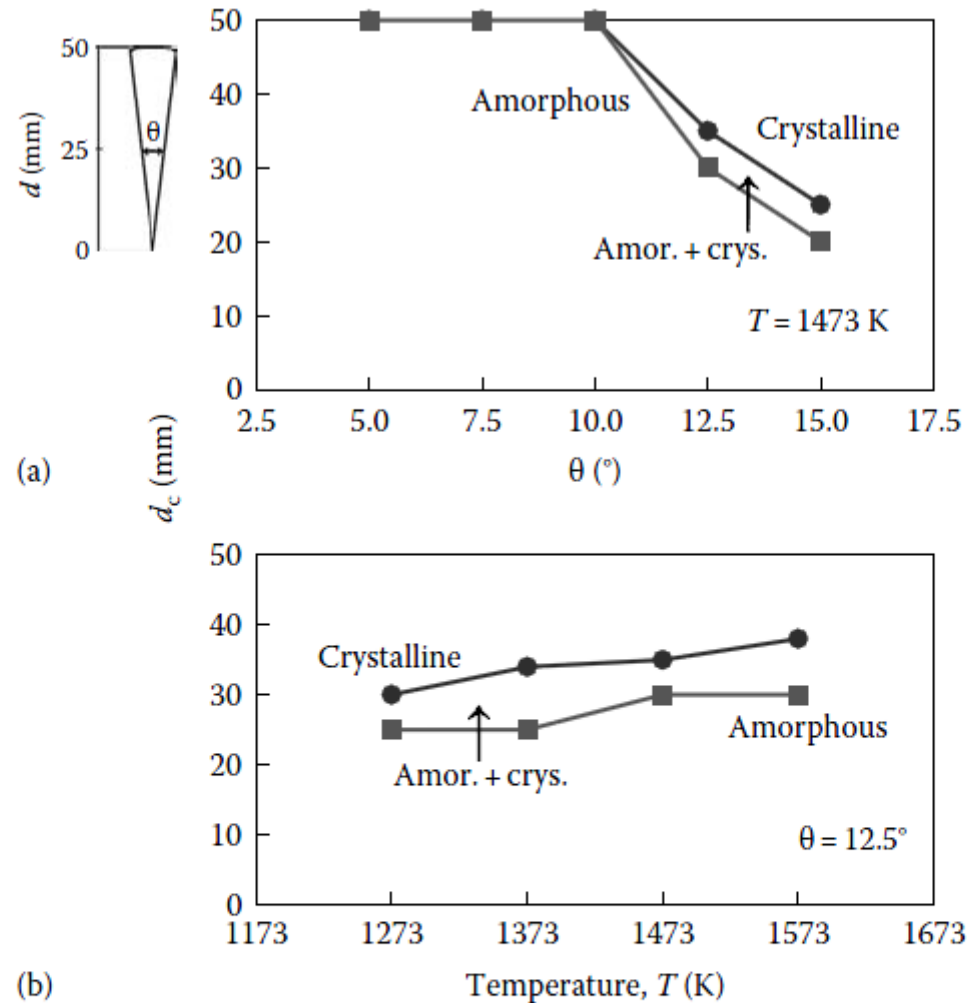


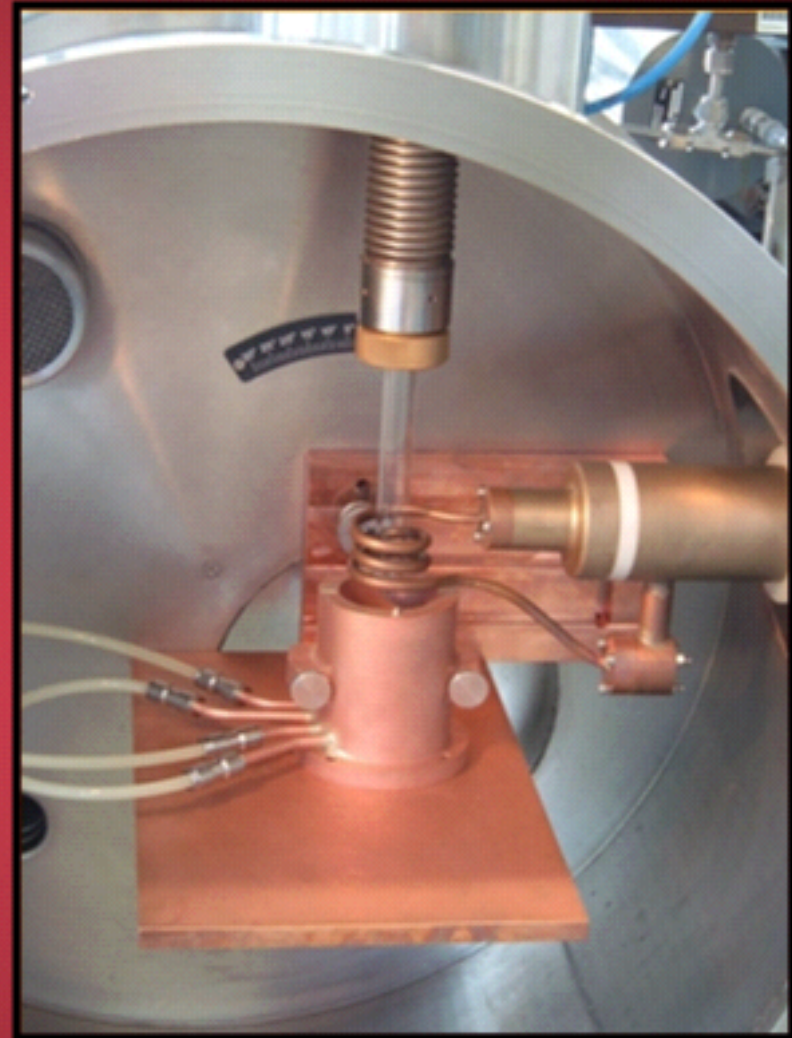
**FIGURE 4.8**

(a) Variation of the constitution of the alloy as a function of the height of the sample from the bottom of the wedge,  $d_c$  and the vertical angle,  $\theta$ . The figure shows the region of formation of the fully glassy phase when the  $Zr_{60}Al_{10}Ni_{10}Cu_{15}Pd_5$  alloy was ejected into the copper mold cavity at a temperature of 1473 K. (b) Variation of  $d_c$  with ejection temperature of the molten metal for the  $Zr_{60}Al_{10}Ni_{10}Cu_{15}Pd_5$  alloy cast into a wedge-shaped mold with a vertical angle  $\theta = 12.5^\circ$ . (Reprinted from Inoue, A. et al., *Mater. Trans., JIM*, 36, 1276, 1995. With permission.)

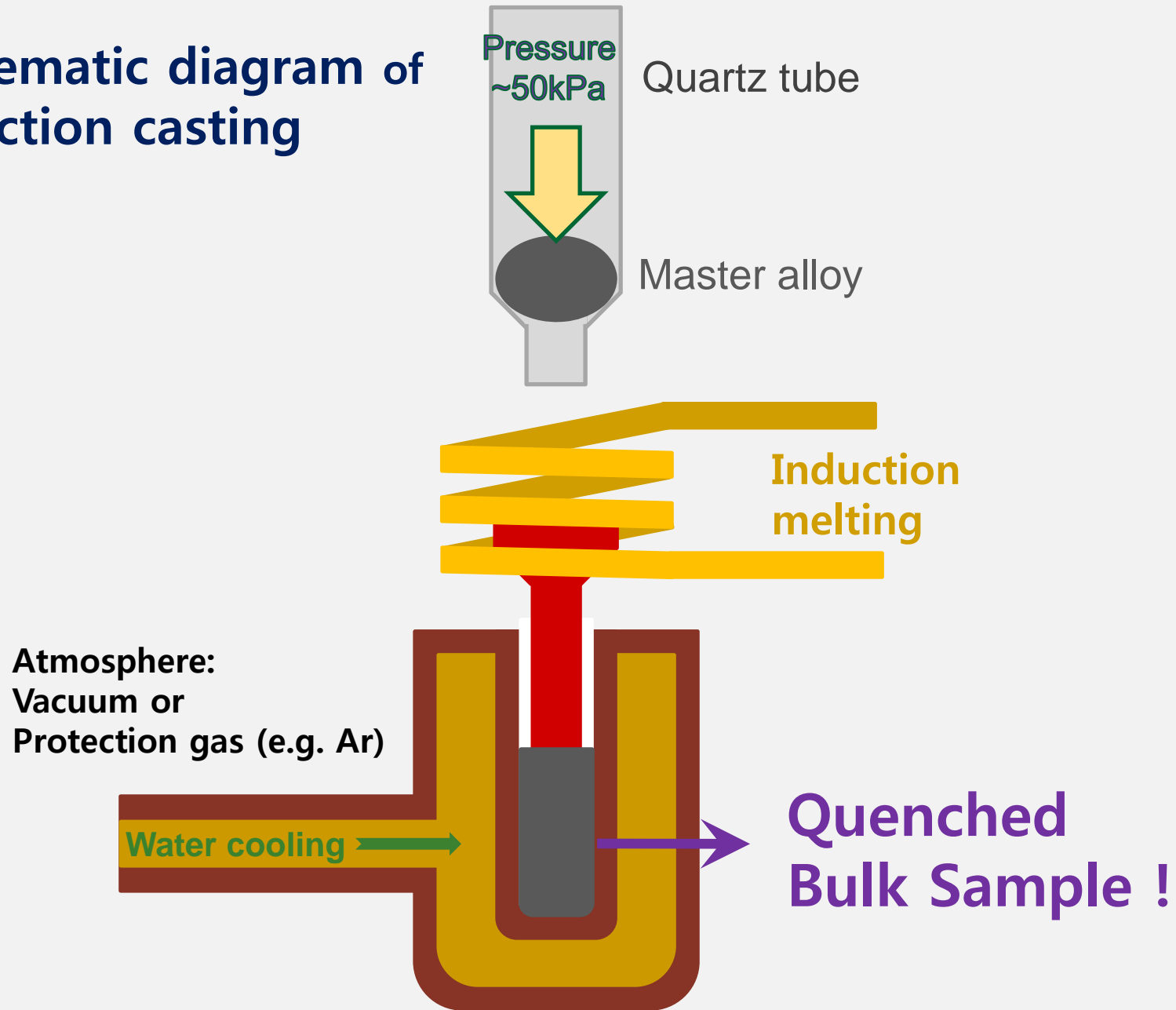
Bulk sample: rod

# Injection casting

- Simple casting method for preparing bulk samples
- Cooling medium :  
Cu mold with water cooling
- Max. cooling rate for rod sample with
  - D=5mm :  $\sim 10$  K/s
  - D=3mm :  $\sim 10^2$  K/s



# Schematic diagram of Injection casting



# Injection cast BMG samples

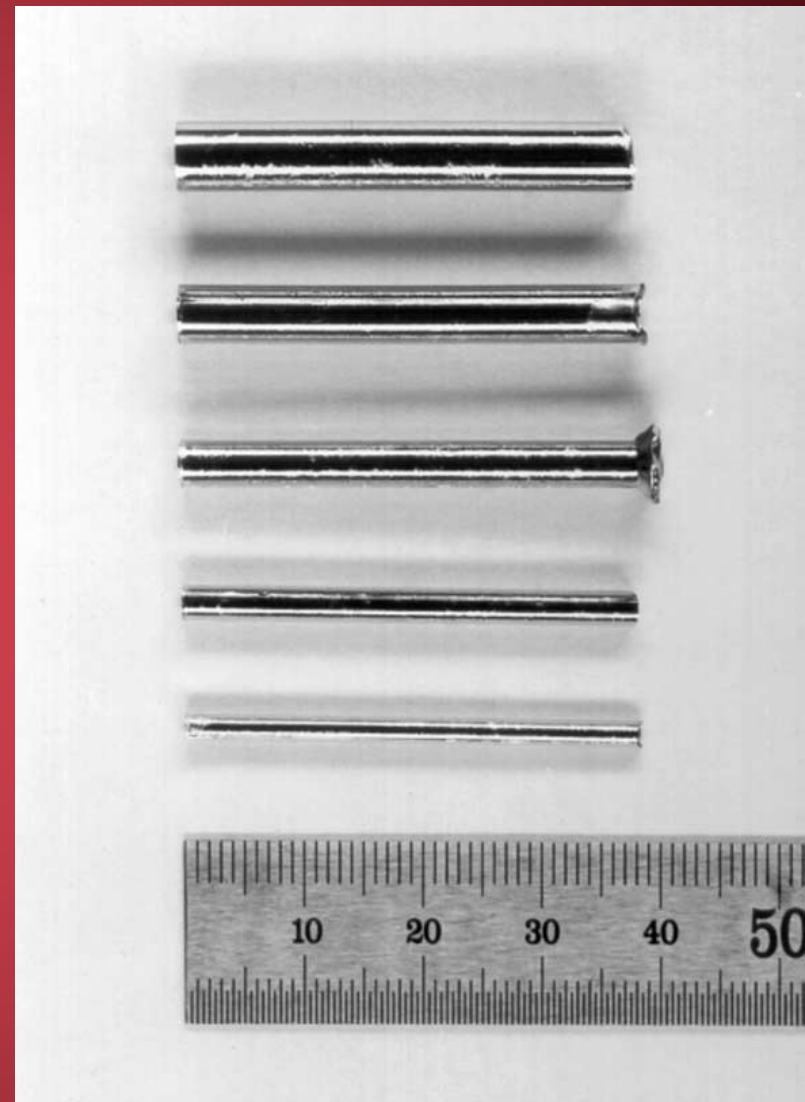
- $\text{Cu}_{47}\text{Ti}_{33}\text{Zr}_{11}\text{Ni}_6\text{Sn}_2\text{Si}_1$   
Alloy samples with diameter from 2 to 6 mm
- Cooling rate can be controlled by changing cavity diameter of mold.
- Cooling rate ( $R_c$ )

$$R_c = K(T_m - T_g)/(r^2 C)$$

$$\cong 10/r^2 \text{ (cm)}$$

K : Thermal conductivity

C : Specific heat capacity



## 4.6 Bulk Metallic Glass Casting Methods

### 4.6.5 Suction-Casting Method

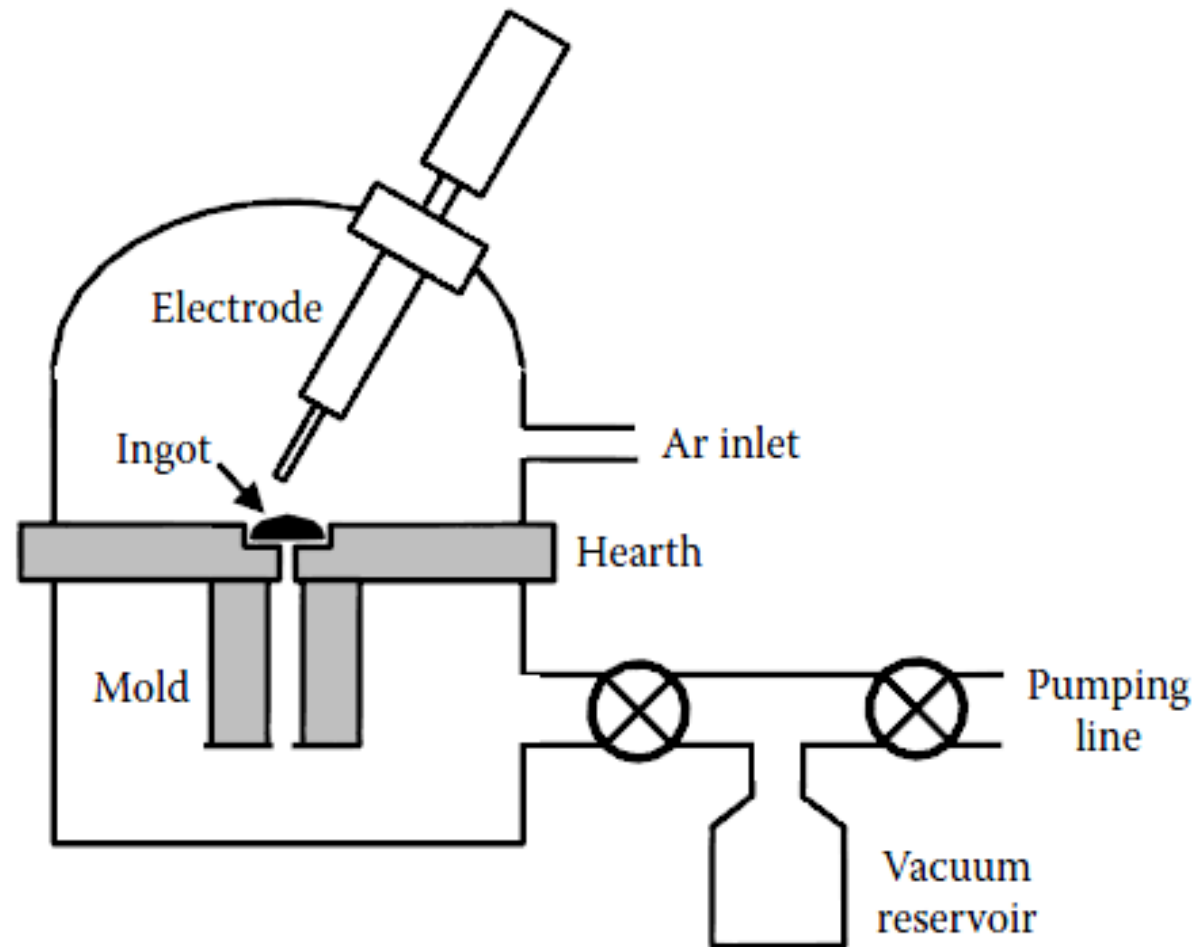
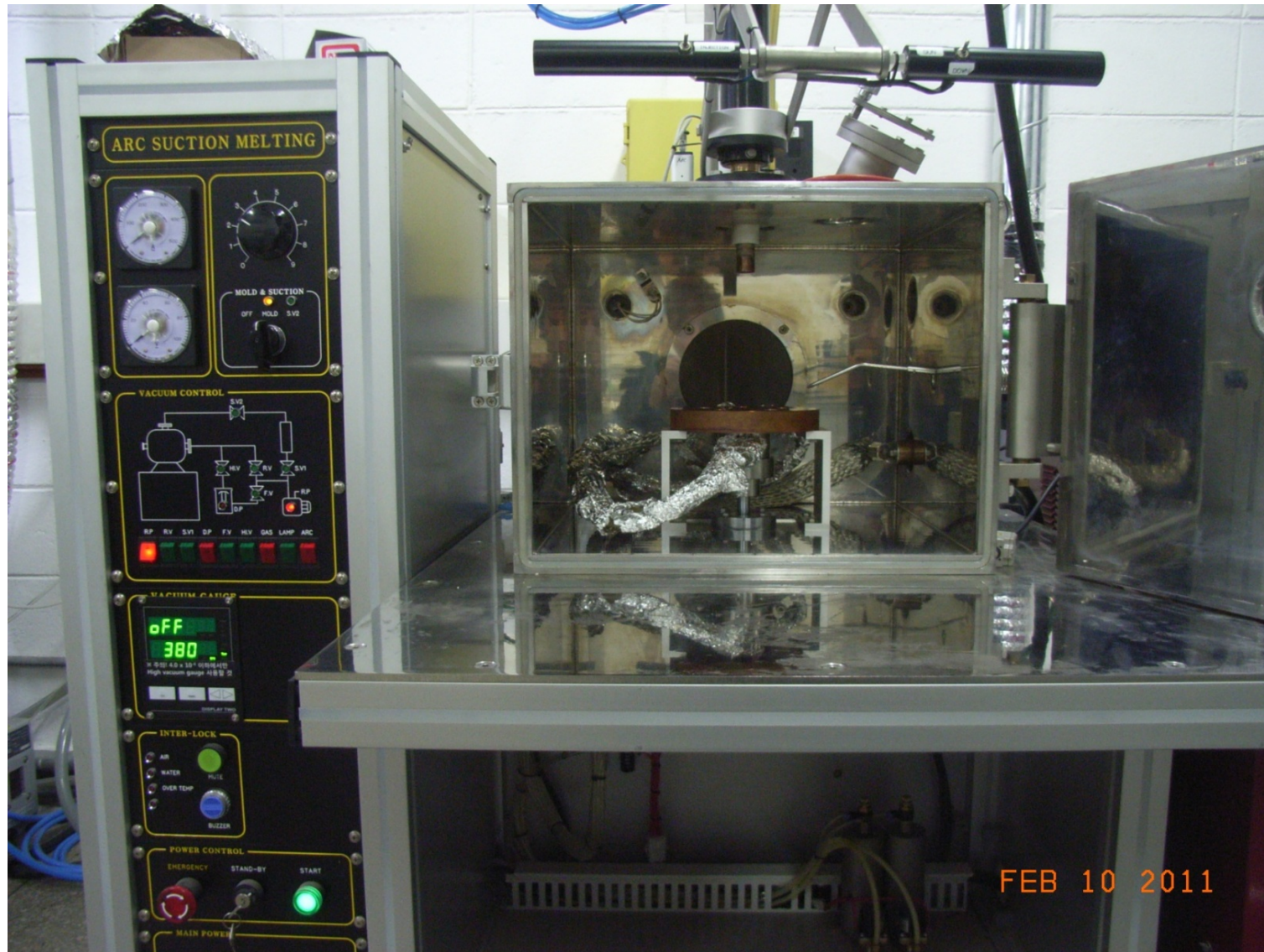


**FIGURE 4.11**

Schematic diagram of the arc melting/suction casting apparatus. (Reprinted from Gu, X. et al., *J. Non-Cryst. Solids*, 311, 77, 2002. With permission.)

Bulk sample: rod

# Suction Casting Method



## Suction Casting Method

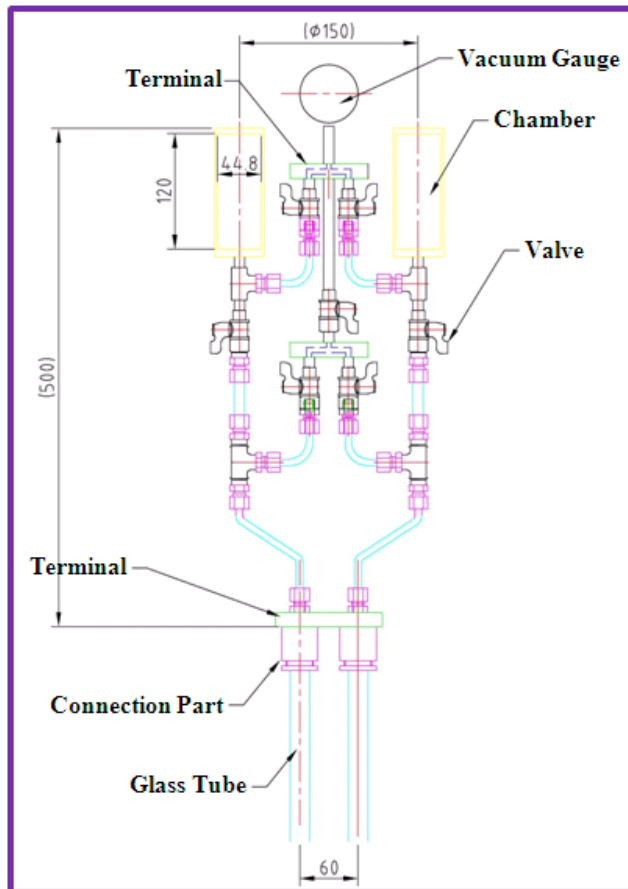
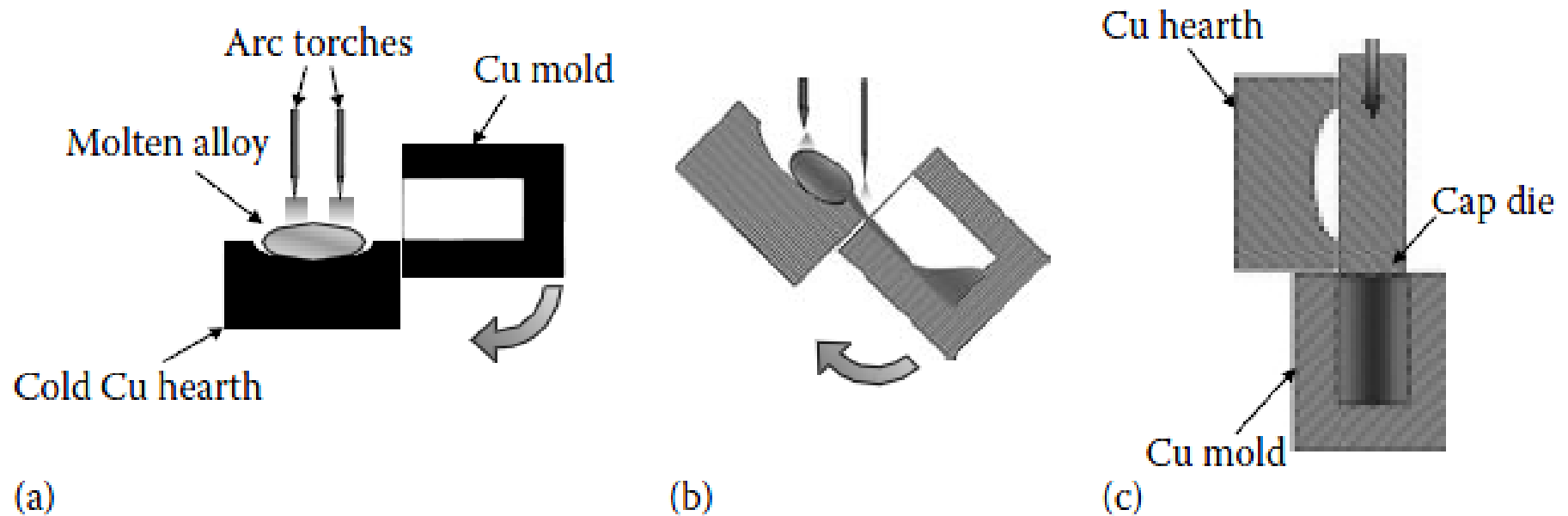


Fig. 6. Photograph of the as-cast specimens of (from left to right):  
(a) suction cast  $12 \times 1 \times \sim 70$  mm<sup>3</sup> plate,  
(b) drop cast  $6.4 \times \sim 70$  mm<sup>2</sup> cylinder,  
(c) suction cast 3 mm diam  $\times \sim 70$  mm cylinder.

## 4.6 Bulk Metallic Glass Casting

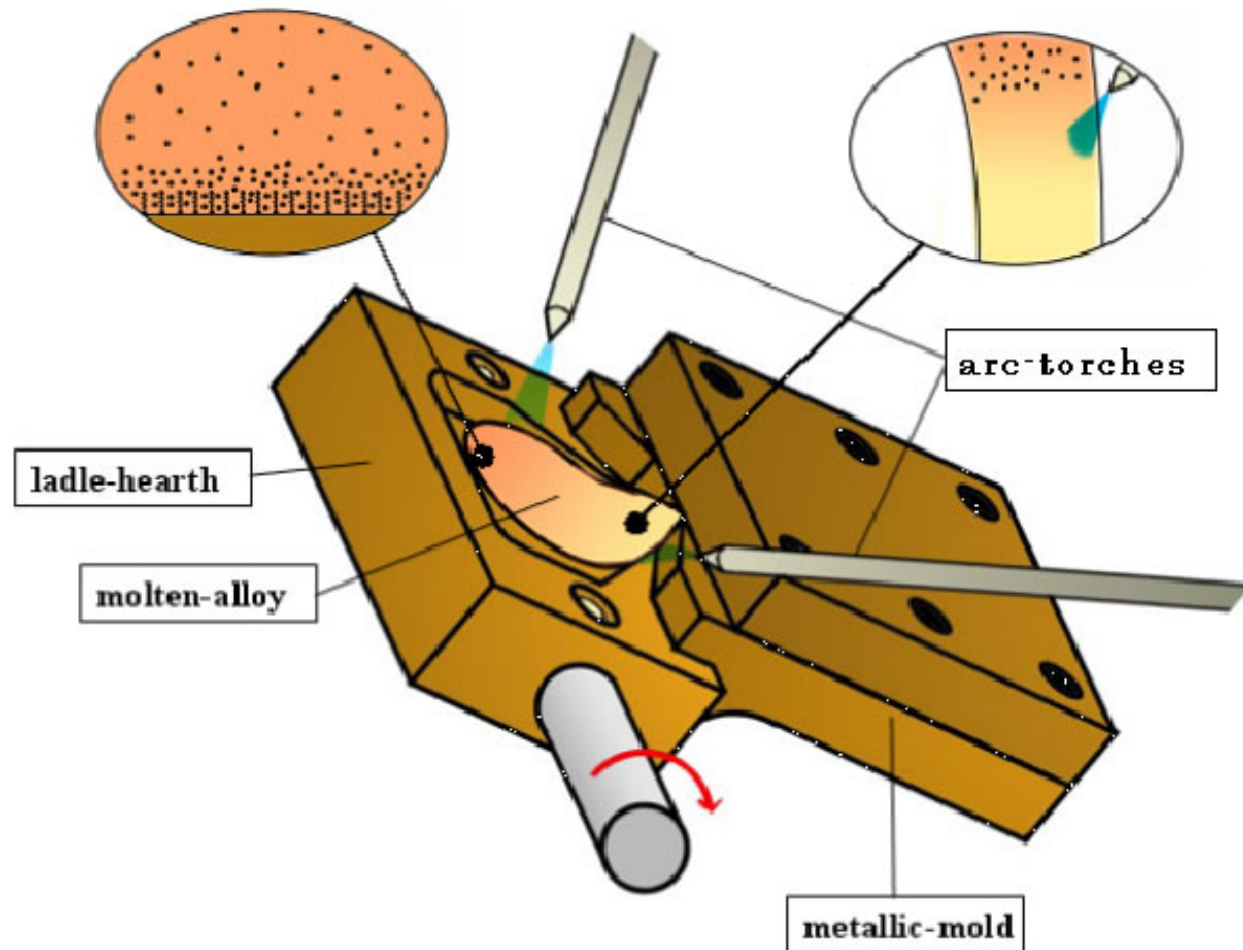
### 4.6.4 Cap-Cast Technique



**FIGURE 4.9**

Schematic diagrams comparing the (a) arc melting, (b) tilt casting, and (c) cap-cast techniques used to produce bulk metallic glassy alloys.

# Fabrication of amorphous materials-tilt casting

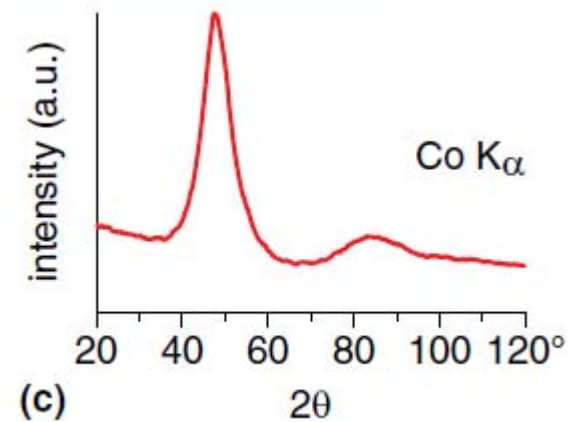
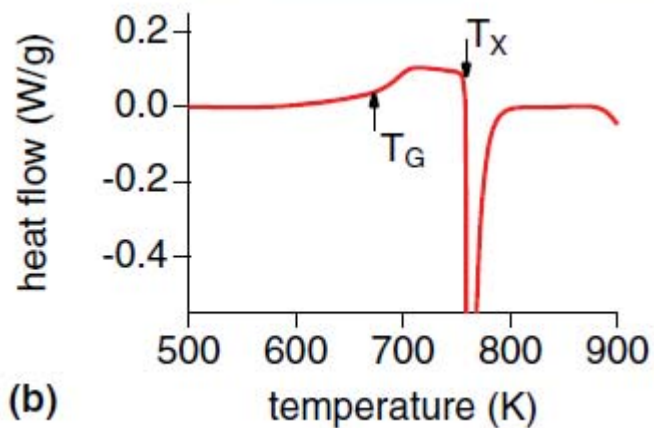


Electric arc: electrical break down of a gas

# Fabrication of amorphous materials-tilt casting

- reduce porosity and inclusions by limiting turbulence
- If the system is rotated slow enough to not induce turbulence, the front of the metal stream begins to solidify.
- If the system is rotated faster then it induces turbulence, which defeats the purpose.

# Fabrication of amorphous materials-tilt casting



Tilt and suction cast specimen with 1,3,5,7,10mm diameters.

Review of scientific instruments 82, 073901(2011)

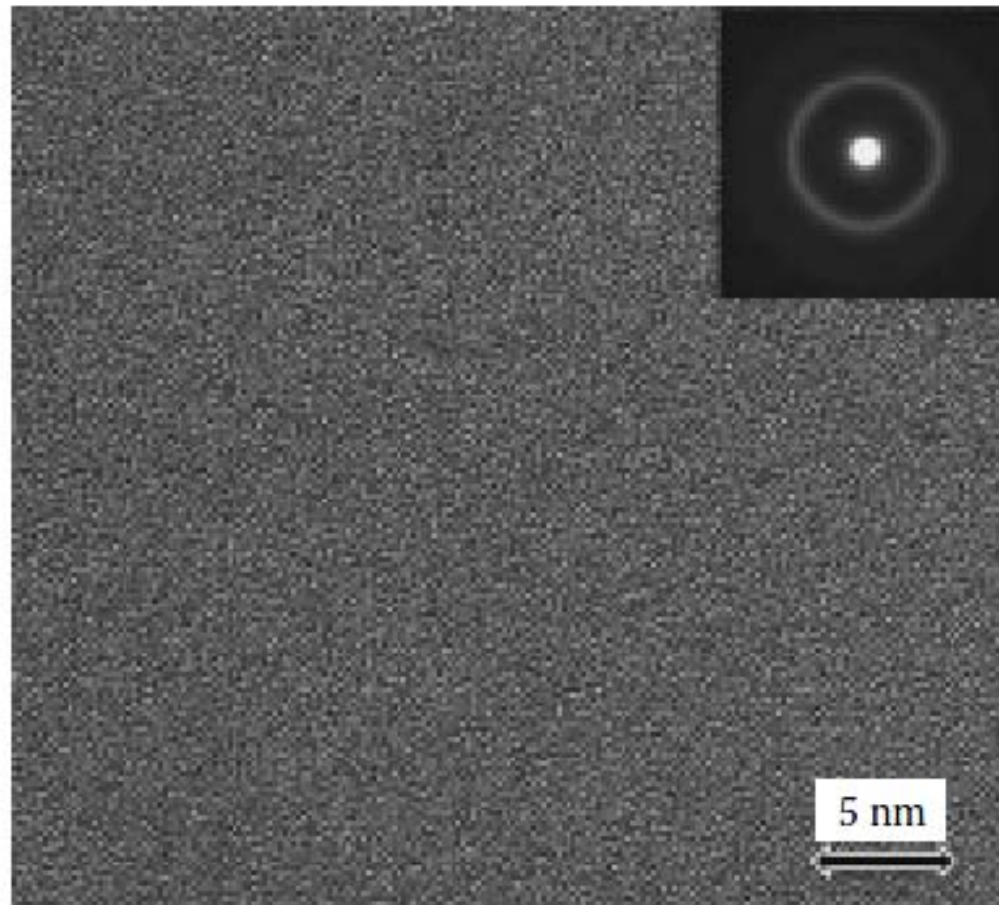


**FIGURE 4.10**

High-resolution transmission electron micrographs of cap-cast  $Zr_{55}Cu_{30}Ni_5Al_{10}$  glassy alloy of 30 mm diameter. The micrograph was recorded from the center of the sample at the site 10 mm from the bottom of the casting. No fringe marks are seen even on a nanometer scale, suggesting that the whole sample was fully glassy.